PACIFIC EARTHQUAKE ENGINEERING RESEARCH CENTER

Reference-Rock Site Conditions for Central and Eastern North America:

Part II – Attenuation (Kappa) Definition

Developed by

NGA-East Geotechnical Working Group

Kenneth W. Campbell
and
Youssef M.A. Hashash, Byungmin Kim, Albert R. Kottke,
Ellen M. Rathje, Walter J. Silva, and Jonathan P. Stewart

Under the Auspices of the
Pacific Earthquake Engineering Research Center

PEER 2014/12
AUGUST 2014

Reference-Rock Site Conditions for Central and Eastern North America:

Part II – Attenuation (Kappa) Definition

Developed by

NGA-East Geotechnical Working Group

Kenneth W. Campbell
and
Youssef M. A. Hashash, Byungmin Kim, Albert R. Kottke,
Ellen M. Rathje, Walter J. Silva, and Jonathan P. Stewart

Under the Auspices of the
Pacific Earthquake Engineering Research Center

Report PEER 2014-12
Pacific Earthquake Engineering Research Center
Headquarters, University of California at Berkeley

August 2014

ABSTRACT

This report presents the results of a comprehensive literature search and limited additional studies that support the recommendation of a probability distribution for the shear-wave (*S*-wave) site attenuation parameter κ_0, or site kappa, associated with a reference-rock site condition in central and eastern North America (CENA). This study was conducted as part of the Geotechnical Working Group (GWG) activities of the Next Generation Attenuation for Central and Eastern North America (NGA-East) Project conducted by the Pacific Earthquake Engineering Research Center (PEER). The recommended reference-rock site condition, which is documented in a separate GWG report, is defined as a hard-rock site with an *S*-wave velocity $\left(V_{s,ref}\right)$ of 3000 ± 300 m/sec [Hashash et al. 2013]. The recommended distribution of the reference-rock site kappa $\kappa_{0,ref}$ for this reference-rock site condition is lognormal, with a median value ($\bar{\kappa}_{0,ref}$) of 0.006 sec, an aleatory standard deviation ($\phi_{\ln \kappa_{0,ref}}$) of 0.43, and epistemic standard deviations ($\varepsilon_{\ln \kappa_{0,ref}}$) of 0.12, when uncertainty in source, path, and site-amplification effects are included in simulations used to develop ground motion prediction equations, and 0.20, when they are not. This distribution is intended to represent the center, body, and range of the technically defensible interpretations of the wider scientific community as defined in the Senior Seismic Hazard Analysis Committee (SSHAC) guidelines [Budnitz et al. 1997; NRC 2012] for a SSHAC Level 3 study. The reference-rock site conditions defined in this study and in Hashash et al. [2013] represent a reference for determining site amplification for other types of site conditions in CENA, a companion activity of the GWG that is being conducted outside of the SSHAC process. One of the major limitations of the study is that most of the data used to estimate κ_0 come from southeastern Canada and the northeastern U.S., and are not necessarily representative of other regions of CENA.

ACKNOWLEDGMENTS

This study was funded by the U.S. Nuclear Regulatory Commission (NRC), U.S. Department of Energy (DOE), and Electric Power Research Institute (EPRI) as part of the Pacific Earthquake Engineering Research Center's (PEER's) Next Generation Attenuation in Central and Eastern U.S. (NGA-East) Project. This support is gratefully acknowledged. Any opinions, findings, and conclusions or recommendations expressed in this material are those of the authors and do not necessarily reflect those of the sponsors. The recommendations provided in this report represent the consensus of the entire NGA-East Geotechnical Working Group and do not represent the opinion of any one individual.

CONTENTS

LIST OF TABLES

LIST OF FIGURES

1 Introduction

The Electric Power Research Institute (EPRI) originally defined a reference-rock site condition in CENA as a midcontinent hard-rock site with an *S*-wave velocity of 2800 m/sec in the top kilometer of the crust and a median κ_0 of 0.006 sec [EPRI 1993]. EPRI used a lognormal distribution to define κ_0 and proposed a natural log standard deviation of 0.40 to define the uncertainty associated with this parameter. However, EPRI eventually used three equally weighted values (0.003, 0.006, and 0.012 sec) to define the total uncertainty in κ_0 in the development of a ground motion prediction equation (GMPE) using the point-source stochastic simulation method [EPRI 1993; Toro et al. 1997].

Later, the U.S. Nuclear Regulatory Commission (NRC) provided the following guidance on the selection of an appropriate $V_{s,ref}$ [NRC 2007]: "The hazard curves from the probabilistic seismic hazard analysis (PSHA) are defined for general surficial rock conditions that are consistent with the definition of rock for the attenuation relationships used in the PSHA. For example, existing attenuation relationships for the central and eastern U.S. (CEUS) typically define generic rock conditions as materials with a shear-wave velocity (V_S) of 2.8 km/sec (9200 ft/sec)." The recommendation of 2.8 km/sec (9200 ft/sec) by the NRC was adopted to maintain compatibility with several existing GMPEs (e.g., Toro et al. [1997]; Somerville et al. [2001]; Silva et al. [2002]; Campbell [2003]; Tavakoli and Pezeshk [2005]; and Atkinson and Boore [2006]) that were being used to estimate ground motions for the reference-rock site conditions defined by EPRI [1993].

The purpose of the present study was two-fold: (1) to review and evaluate—within the framework of a SSHAC Level 3 process—the data and studies that have been conducted since the original 1993 EPRI report was released; and (2) to recommend whether the distribution of $\kappa_{0,ref}$ for a reference hard-rock site in CENA should be revised. As will be shown later, the recommended median value of $\kappa_{0,ref}$ is the same as that originally proposed by EPRI [1993]; however, the distribution and total standard deviation of this parameter have been modified. Furthermore, the total uncertainty in $\kappa_{0,ref}$ has been separated into its aleatory (randomness) and epistemic (lack of scientific knowledge) components, consistent with the characterization of uncertainty in contemporary U.S. and international guidelines on PSHA methodology for civil and nuclear facilities (e.g., McGuire [2004]; NRC [2007]; ANSI [2008]; IAEA [2010]; DOE [2011]; and NRC [2012]). One of the major limitations of the study is that most of the data used to estimate κ_0 come from southeastern Canada and the northeastern U.S., and are not necessarily representative of other regions of CENA.

2 The Origins and Definition of Site Kappa

Seismologists have long recognized that the amplitude decay of seismic waves within the Earth's crust, defined herein as the effective attenuation of shear waves (*S*-waves) [Lay and Wallace 1995; Sato et al. 2002], can be approximated by an equation of the form (e.g., Futterman [1962] and Knopoff [1964])

$$A(r, f) = A_0 \exp(-\pi fr / Q_{ef} V_S) \quad (1)$$

where *r* is distance, *f* is frequency, Q_{ef} is the effective seismic quality factor of *S*-waves (inverse of seismic attenuation), and V_S is the *S*-wave velocity of the medium. Seismic attenuation can be thought of as either the fractional loss of energy per cycle of oscillation (e.g., Lay and Wallace [1995]) or the exponential decrease in amplitude with time or distance [Frankel and Wennerberg 1987]. It has traditionally been divided into two components: a frequency-independent component commonly referred to as intrinsic attenuation or anelasticity (Q_{in}^{-1}), which results from friction or internal damping, and a frequency-dependent component commonly referred to as scattering attenuation (Q_{sc}^{-1}), which results from heterogeneities (scatterers) along the travel path [Aki 1980]. Dainty [1981] showed that the effective attenuation can be thought of as the sum of these two attenuation components:

$$Q_{ef}^{-1} = Q_{in}^{-1} + Q_{sc}^{-1} \quad (2)$$

Therefore, if Q_{sc} is frequency dependent and significantly contributes to the effective attenuation, then Q_{ef} also will be frequency dependent. Although this attenuation paradigm was developed from surface recordings and applied to attenuation in the lithosphere, Abercrombie [1998] and Kinoshita [2008] have shown that it apparently also applies to borehole recordings.

Recently, Morozov [2008; 2009] has questioned the current attenuation paradigm and suggests that the distinction between a frequency-independent Q_{in} and a frequency-dependent Q_{sc} is confusing and misleading, especially in the context of Equation (1). He proposed an alternative geometrical attenuation model to replace the conventional frequency-dependent attenuation law commonly defined by the power-law function, $Q(f) = Q_0 (f / f_0)^{\eta}$. The new model provides a straightforward differentiation between geometrical and effective attenuation, with the traditional scattering attenuation interpreted in terms of a generally frequency-independent component of geometrical attenuation and an effective attenuation, which he calls Q_e (not to be confused with the effective attenuation Q_{ef} defined in this study) that incorporates the frequency-independent component of intrinsic attenuation and small-scale scattering. Unlike the (Q_0, η) description of attenuation, the inversion procedure proposed by Morozov uses only the spectral amplitude data and does not rely on "elaborate theoretical models or restrictive assumptions." Data from over 40 reported studies were transformed to this new parameterization. The levels of geometrical attenuation were found to strongly correlate with crustal tectonic types and decrease with tectonic age. The corrected values of Q_e were found to be frequency independent and generally significantly higher than Q_0, and showed no significant correlation with tectonic age. Several case studies were revisited in detail, including one involving the deep borehole data of Kinoshita [2008], with significant changes in the interpretations. Since Morozov's [2008; 2009] conclusions have not yet been fully vetted by the seismological community, the conventional distinction between these two attenuation mechanisms is continued to be made in this paper. However, like Morozov [2008; 2009], the combined intrinsic and scattering attenuation data is interpreted in terms of a single frequency-independent quality factor Q_{ef}.

It was not until the early 1980s with the refinement of the stochastic ground motion simulation method (see Boore [1983] and references therein) that it was recognized that whole-path attenuation within the crust could not completely explain the decay of high-frequency acceleration spectra beyond the source corner frequency, where the acceleration spectrum should be flat according to the commonly accepted ω-square source displacement spectrum [Brune 1970; 1971]. Hanks [1982] suggested that this observed cut-off frequency, which he called $f_{\max}$, was likely the result of site attenuation. Papageorgiou and Aki [1983] suggested that it was primarily a source effect. Without judging which interpretation was correct, Boore [1983] included the effect of this cut-off frequency in his generalization of the stochastic ground motion simulation method of Hanks and McGuire [1981] by including a high-cut filter in his model of the Fourier acceleration spectrum given by the equation

$$D(f) = [1 + (f / f_{\max})^8]^{-1/2} \quad (3)$$

Around the same time that Hanks [1982] and Papageorgiou and Aki [1983] were debating whether $f_{\max}$ was a site attenuation parameter or a source parameter, Cormier [1982] proposed a model in which seismic attenuation could be defined by the rate of the high-frequency decay of the displacement spectrum for frequencies above the corner frequency as the multiplication of two terms: (1) the decay due to the source spectrum, f^{-n}; and (2) an exponential decay factor due to attenuation, $\exp(-\pi t^* f)$. In this model, t^* represents the path-integrated effect of the inverse of the quality factor as defined by the integral [Kanamori 1967]:

$$t^* = \int_{\text{path}} Q_{ef}(r)^{-1} V_S(r)^{-1} dr \quad (4)$$

Cormier also noted that experimental measures of t^* typically lump scattering effects together with intrinsic anelasticity and combine frequency-dependent attenuation mechanisms together with frequency-independent attenuation mechanisms. Therefore, t^* provides a measure of Q_{ef} rather than Q_{in} or Q_{sc}.

After studying the high-frequency decay of accelerograms recorded in California, Anderson and Hough [1984] suggested that the shape of the acceleration spectrum at high frequencies can be described by an equation similar to Cormier's [1982] as given by the equation

$$A(f) = A_0 \exp(-\pi\kappa f), \qquad f > f_E \tag{5}$$

where the amplitude A_0 depends on factors such as source properties and propagation distance, κ is a spectral decay parameter, and f_E is a frequency beyond which the falloff of the spectrum is approximately linear on a plot of the logarithm of $A(f)$ versus f (see Figure 1. According to this equation, the slope of the spectral decay, $\mathrm{d}\ln A(f)/\mathrm{d}f$, is equal to $-\pi\kappa$. Anderson and Hough [1984] noted that if $Q_{ef}(r)$ and thus t^* is independent of frequency, the effect of attenuation on a Brune source displacement spectrum [1970; 1971], for which the high-frequency decay is proportional to f^{-2}, will yield the spectral shape given by both Cormier [1982] and Equation (5). These authors further found that κ was dependent on distance with a nonzero intercept that they interpreted to be the attenuation due to the propagation of *S* waves through the subsurface geological structure and a slope that they interpreted to be the incremental attenuation due to the horizontal propagation of *S* waves through the crust. They also showed that the spectral decay of the logarithm of the Fourier acceleration spectrum with frequency, assuming an ω-square source spectrum, is flat (i.e., $\kappa = 0$) when $Q_{ef} = \infty$ or $Q_{ef} \propto f$, and is negative (i.e., $\kappa > 0$) when $Q_{ef} = Q_0$ or $Q_{ef} \propto f^{\eta}$ ($\eta < 1$). However, only if $Q_{ef} = Q_0$ (a constant) is the spectral decay described exactly by Equation (5). Fitting Equation (5) to a model with a fractional frequency dependence of Q_{ef} will yield a smaller value of κ than a model in which Q_{ef} is assumed to be constant, which emphasizes the importance of the standard assumption that Q_{ef} is independent of frequency when interpreting κ as a site parameter. Otherwise, the true value of Q_{ef} will be underestimated.

Hough et al. [1988] and Hough and Anderson [1988] performed a thorough study of κ using the recordings of small earthquakes from the Anza seismic array in southern California. Based on this analysis, Hough and Anderson [1988] proposed a general model for κ given by the equation

$$\kappa(r) = \int_{\text{path}} Q_i(z)^{-1} V_S(z)^{-1}\, dr \tag{6}$$

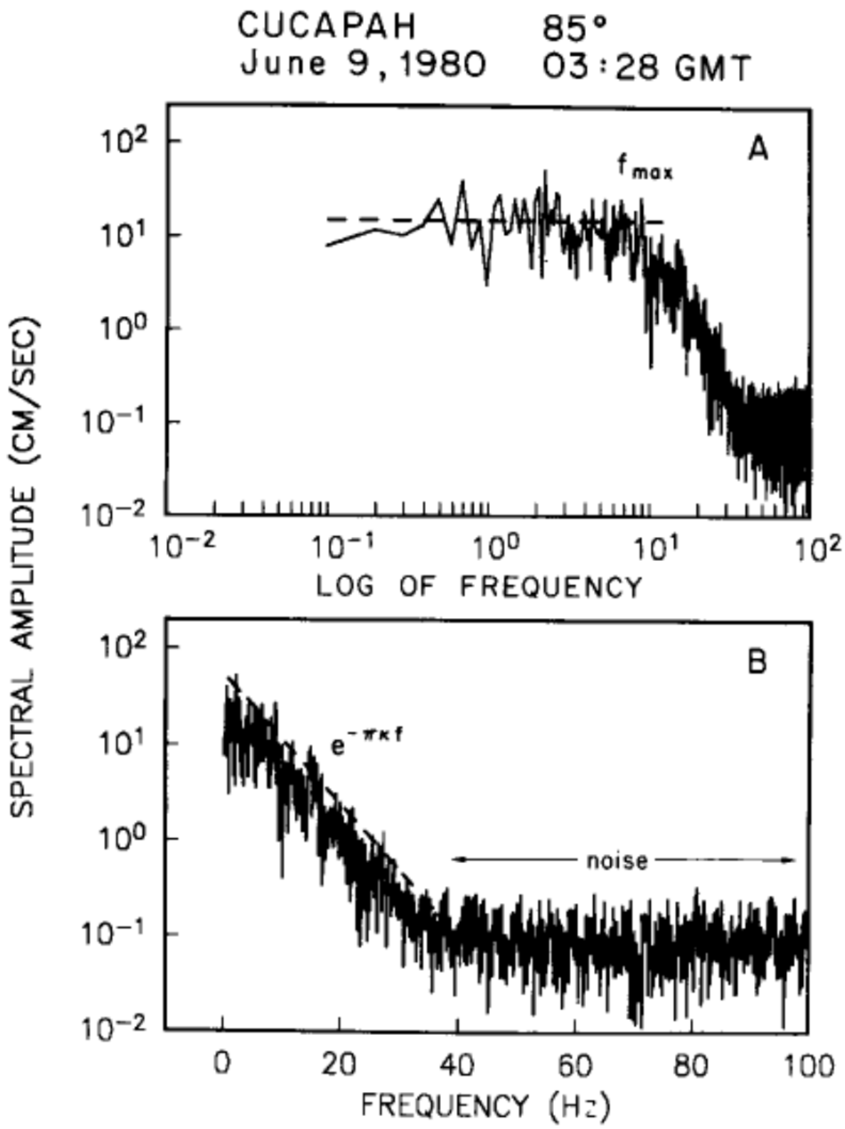

Figure 1 **Illustration showing the definition of κ for the Fourier amplitude spectrum of the N85°E component of ground acceleration recorded at Cucapah during the Mexicali Valley earthquake of June 9, 1980 (M_L 6.2). The accelerograph was a digital recorder that samples at a rate of 200/sec. (A) log-log axes; and (B) linear-log axes (after Anderson and Hough [1984]).**

where Q_i is the frequency-independent component of Q_{ef} at depth z within the profile. They used this model to infer the attenuation structure at Anza from a regional crustal velocity model. They noted that their proposed model for $\kappa(r)$ was the same as that given by Cormier [1982] for $t*$ in Equation (4), except that it used only the frequency-independent component of Q_{ef}. Hough et al. [1988] concluded that the similarity of the distance-dependence of $\kappa(r)$ in the Anza and Imperial Valley regions of southern California, areas in which the intercepts at $r = 0$ were very different and presumably due to the vastly different subsurface geology, supported the earlier assumption by Anderson and Hough [1984] that the intercept of $\kappa(r)$ represents the attenuation of seismic waves within the geological structure beneath the site, and that the distance-dependence of $\kappa(r)$ represents the attenuation due to the horizontal propagation of seismic waves within the crust. Hough et al. [1988] referred to this site component of $\kappa(r)$ as κ_0, which is the term used in this report. Anderson [1991] generalized the linear $\kappa(r)$ model of Hough and Anderson [1988] and Hough et al. [1988] by proposing a mathematical formulation of the observed behavior of κ that treated this parameter as an arbitrary function of distance, which he defined by the equation

$$\kappa(r) = \kappa_0 + \tilde{\kappa}(r) \tag{7}$$

where κ_0 (site kappa) is the intercept at $r = 0$.

Since its introduction, κ_0 has become the preferred parameter for incorporating site attenuation in the calculation of amplification factors using the quarter-wavelength method of Joyner et al. [1981]. A summary of κ_0 estimates for a variety of geological conditions throughout the U.S. is given by Anderson [1986; 1991] and Silva and Darragh [1995]. Even Halldorsson and Papageorgiou [2005] have adopted it as their high-frequency filter parameter in the revision of the specific barrier model of the earthquake source [Papageorgiou and Aki 1983] because of its better fit to strong-motion data. However, these latter authors continue to suggest that it could be a source parameter rather than a site parameter.

In the quarter-wavelength method, the site amplification of the Fourier amplitude spectrum of acceleration is calculated from the equation [Boore 2003]

$$Amp(f) = (\rho_S \beta_S / \bar{\rho}\bar{\beta})^{1/2} \exp(-\pi \kappa_0 f) \tag{8}$$

where ρ_S and β_S are the density and *S*-wave velocity at the base of the geological profile and $\bar{\rho}$ and $\bar{\beta}$ are the time-averaged density and *S*-wave velocity over a depth equivalent to the quarter wavelength of a seismic wave of frequency *f* propagating vertically through the profile. The important effect of κ_0 on $Amp(f)$ is demonstrated in Figure 2. All of the CENA ground motion estimates used in the 2008 update of the national seismic hazard maps [Petersen et al. 2008] have either been directly or indirectly adjusted to NEHRP site class B/C site conditions [BSSC 2009] using this equation. Therefore, the discussion of Q_{ef} and κ_0 presented in the remainder of this paper is confined to their use in the quarter-wavelength method. Campbell [2009] discusses how conclusions regarding these attenuation parameters could be quite different in the context of other more complex site amplification methods.

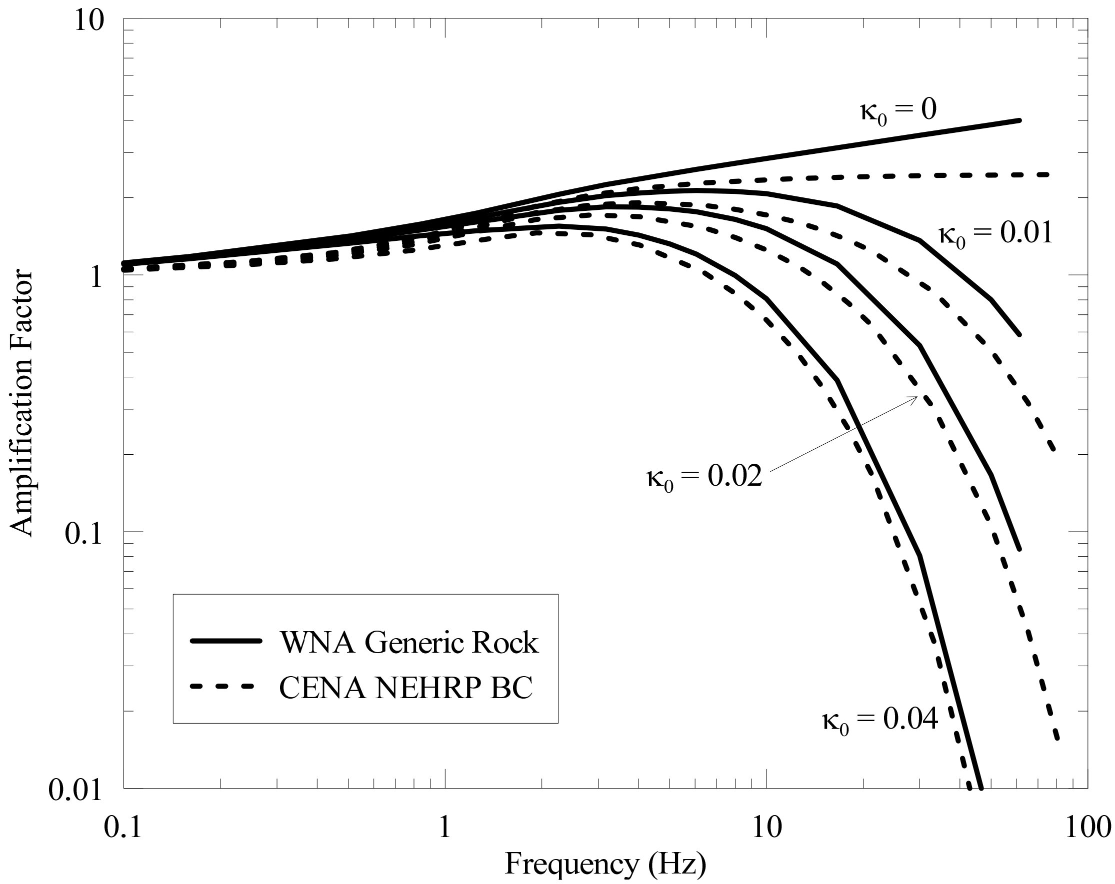

Figure 2 **Site amplification of Fourier amplitude spectra for the WNA generic-rock profile of Boore and Joyner [1997] and the hypothetical CENA BC site profile of Frankel et al. [1996]. Site factors were calculated using the quarter-wavelength method [Joyner et al. 1981; Boore 2003]. The different curves show the effect of the site attenuation parameter κ_0 (sec).**

3 Methods Used to Estimate Site Kappa

The values of κ_0 summarized in this report were estimated using two fundamental approaches. The first approach is based on identifying a value, f_{max}, at which the Fourier amplitude spectrum of acceleration begins to decay rapidly at high frequencies [Hanks 1982]. Later, Boore [1986] showed that f_{max} could be used to estimate κ_0 from the relationship $f_{\max} = 1/(\pi\kappa_0)$, thus providing a means of relating these two site attenuation parameters. This relationship was used to estimate κ_0 for those studies that reported estimates of f_{max} for CENA [Atkinson 1984; Toro and McGuire 1987].

The second approach used to estimate the values of κ_0 summarized in this report is based directly on the original definition of kappa by Anderson and Hough [1984] and latter refined by Hough and Anderson [1988], Hough et al. [1988], and Anderson [1991]. This approach assumes that the linear trend in the log-linear plot of the Fourier amplitude spectrum of acceleration for frequencies above the corner frequency of the source spectrum, as defined in Equation (8), can be used to estimate the attenuation beneath the site based on a site attenuation operator given by the function $\exp(-\pi\kappa_0 f)$, where f is frequency (Hz). Subclasses of this approach include:

- fitting response spectral templates to the observed response spectra using simple, usually stochastic, models of the source, path, and site-amplification effects beneath the site [Silva and Darragh 1995]
- performing inversions of the observed Fourier amplitude spectra of ground motion using simple stochastic models (e.g., Atkinson [1996]; Chapman et al. [2003]; Bay et al. [2005]; Atkinson and Boore [2006]; and Campbell [2009])

In each subclass, all of the seismological and geological parameters required to define the source, path, and site-amplification effects are taken from other regional studies (response spectral fitting approach) or from inversions of the same set of recordings that are used to derive κ_0 (Fourier inversion approach).

A subclass of the Fourier inversion approach fits either a linear [Anderson and Hough 1984] or non-parametric [Anderson 1991] curve directly to the distance dependence of kappa instead of including a source or path attenuation term in the simulation and determines the site component of kappa (κ_0) as the intercept of this curve at zero distance. This approach has not been applied in CENA, but it has been applied extensively in California [Anderson and Hough

1984; Hough and Anderson 1988; Hough et al. 1988; Anderson 1991; Van Houtte et al. 2011], Europe [Castro et al. 2000; Drouet et al. 2010; Edwards et al. 2011; Gentili and Franceschina 2011; Van Houtte et al. 2011], Japan [Oth et al. 2011; Van Houtte et al. 2011], and Mexico [Purvance and Anderson 2003].

4 Site Kappa for Hard-Rock Sites in CENA

Available estimates of κ_0 for hard-rock sites in CENA (except for carbonate platform regions which are common in the Midwest region of North America) are summarized in Table 1. Atkinson [1984] found that near-source recordings of the 1982 Miramichi, New Brunswick, aftershocks in eastern Canada were consistent with a f_{max} in the range of 35 to 50 Hz. She also noted that Fourier amplitude spectra obtained from seismographs close to the 1983 Ottawa earthquake swarm implied a f_{max}, if it exists (her words), greater than 30 Hz (Hasegawa, personal communication). On the basis of these limited data, she assumed that a f_{max} of 50 Hz was a conservative first approximation for eastern Canadian earthquakes. This value was later used by Boore and Atkinson [1987] to develop a hard-rock GMPE for hard-rock sites in CENA. It corresponds to a κ_0 of approximately 0.0064 sec, using the approximate relationship $f_{max} \approx 1/\pi\kappa$ proposed by Boore [1986] for small and moderate earthquakes. The lower bound f_{max} of 35 Hz corresponds to an approximate κ_0 of 0.0091 sec. Toro and McGuire [1987] proposed an f_{max} of 40 Hz, corresponding to an approximate κ_0 of 0.0080 sec, after reviewing near-field aftershock recordings of the New Brunswick earthquake. Silva and Green [1989] found that this latter value resulted in spectral shapes predicted by the point-source stochastic simulation method that were reasonably consistent with the available strong ground motion data in CENA.

Darragh et al. [1989] found an average κ_0 of 0.006 sec for hard-rock sites in CENA using the response spectral fitting approach. Silva and Darragh [1995] used the response spectral fitting approach together with the point-source stochastic simulation method to derive empirical estimates of κ_0 for 16 strong-motion recordings for CENA hard-rock sites described as granitic plutons, carbonates, and Precambrian rock of the Canadian Shield. They used the band-limited white-noise simulation method of Boore [1983] with a single-corner source spectrum [Brune 1970; 1971], a 100-bar stress drop, a constant r^{-1} geometrical attenuation model, a frequency-dependent crustal Q model given by $Q(f) = 500 f^{0.65}$, and a site amplification model given by Equation (8). Using this model, they found a median κ_0 of 0.007 sec with individual estimates that ranged from 0.004–0.016 sec. The upper end of this range decreases to 0.008 sec if the problematic Monticello Reservoir, South Carolina, sites are removed (see discussion below), giving a median value closer to 0.006 sec. The results of these studies were used by EPRI [1993], Toro et al. [1997], and Silva et al. [2002] to select a median κ_0 of 0.006 sec in their development of hard-rock ground motion prediction equations for CENA.

Table 1 Summary of hard-rock site kappa (κ_0) estimates in CENA.

Source	Mean (sec)	Range (sec)	Comments
Atkinson [1984]	0.006	–	Based on $f_{\max} = 50$ Hz
Atkinson [1984]	0.009	–	Based on $f_{\max} = 35$ Hz
Toro and McGuire [1987]	0.008	–	Based on $f_{\max} = 40$ Hz
Darragh et al. [1989]	0.006	–	–
Silva and Darragh [1995]	0.007	0.004 – 0.016	Including Monticello Res.
Silva and Darragh [1995]	0.006	0.004 – 0.008	Excluding Monticello Res.
Atkinson [1996]	0.002	0 – 0.004	4 – 30 Hz
Chapman et al. [2003]	0.009	0 – 0.018	Monticello Reservoir
Campbell [2009]	0.004	0 – 0.007	12 – 22 Hz [Atkinson 1996]
Atkinson and Boore [2006]	0.005	0 – 0.01	Data from Atkinson [2004]

Atkinson [1996] proposed an upper-bound value of 0.004 sec for the Canadian Shield based on the spectral decay of Fourier acceleration spectra over frequencies of 4–30 Hz from small earthquakes recorded on the Eastern Canadian Telemetered Network (ECTN). Based in part on this study, Beresnev and Atkinson [1999] used a median κ_0 of 0.002 sec in their estimation of hard-rock ground motions using a finite-source stochastic simulation model. However, these authors also used a site amplification factor of unity, which is consistently smaller than contemporary estimates (e.g., Atkinson and Boore [2006]), and an adjustable high-frequency strength factor, both of which likely compensated for the use of a relatively small κ_0 value. Close inspection of Atkinson's [1996] Figure 7 suggests that κ_0 could be as high as 0.007 sec over the 12–22 Hz frequency range for which the observed spectral decay appears to be less impacted by possible high-frequency noise and low-frequency source and site-amplification effects. It is also possible that the ECTN sites in the Canadian Shield, which are generally sited on a thin layer of till or weathered rock over hard, glacially scoured Precambrian rock [Beresnev and Atkinson 1997] are underlain by higher quality rock than the average hard-rock site used by Silva and Darragh [1995].

Anderson and Hough [1984], Anderson [1986; 1991], Anderson et al. [1996], and Barton [2007] show that the rock quality and the quality factor of the rock can have a significant impact on material damping and, therefore, κ_0. In fact, numerical site-response simulations by Anderson et al. [1996] suggest that the quality factor within the site profile is of equal importance to that in the upper-most layer in determining the amount of amplification at high frequencies and more important than the *S*-wave velocity in these layers. A specific example for CENA is given by Atkinson [1996], who found relatively large κ_0 values of 0.02–0.04 sec for ECTN sites in the Charlevoix and Sudbury areas of southeastern Canada, which are reportedly located on fractured Precambrian rock within an ancient meteor impact crater. Similarly, Silva and Darragh [1995] found a κ_0 of 0.025 sec from strong-motion recordings of the 1988 Nahanni, Northwest Territories, earthquake sequence on a site described as "sheared rock." These later results are also consistent with the results of laboratory experiments on hard-rock specimens that have shown that the more fractured the rock the lower the quality factor (e.g., Johnston et al. [1979]; Johnston and Toksov [1980]; Barton [2007]).

In an attempt to estimate κ, Chapman et al. [2003] analyzed the spectral decay of 25 recordings located approximately 10 km from a swarm of 23 very shallow (0.1–2.4 km deep) microearthquakes with magnitudes ranging from 0.1 to 1.2 at Monticello Reservoir, South Carolina. Because of the short distances and low attenuation, these estimates are approximately equivalent to κ_0. The earthquakes and the recording site were located within a complex metamorphic terrain intruded by plutons of granite and granodiorite composition. They used a response spectral fitting technique similar to that of Silva and Darragh [1995] to determine a median κ that ranged from –0.004 to 0.018 sec for upper frequency limits ranging from 15 to 40 Hz (the high-frequency limit of the data). They attributed the higher values of κ to a bias caused by the relatively low (15–25 Hz) corner frequencies of the earthquakes and concluded that the true value of κ_0 was too small to be resolvable from the data (i.e., $\kappa_0 \leq 0.01$ sec). Silva and Darragh [1995] interpreted several microearthquake seismograms at Monticello Reservoir recorded at epicentral distances of 1–8 km to infer a κ_0 of 0.013–0.016 sec, which is near the upper range of the values derived by Chapman et al. [2003] and possibly subject to the same biases noted by these investigators.

Atkinson and Boore [2006] carefully examined the Fourier acceleration spectra compiled by Atkinson [2004] and found that these data were consistent with individual estimates of κ_0 that ranged from 0 (no attenuation) to 0.01 sec with a median value of 0.005 sec. The database consisted of 1700 digital seismograms from 186 earthquakes (m_N 2.5–5.6) that occurred in southeastern Canada and northeastern U.S. from 1990 to 2003. These data were recorded by short-period ECTN seismographs and by broadband seismographs of the Canadian National Seismographic Network (CNSN) and the U.S. National Seismic Network (USNSN) on hard-rock sites that were reported to have near-surface *S*-wave velocities in excess of 2000 m/sec [Beresnev and Atkinson 1997].

5 Site Kappa for Hard-Rock Sites in WNA

In order to show that the small values of κ_0 reported for CENA hard-rock sites in the preceding section are not unrealistic, it is useful to compare them with estimates for hard-rock sites in western North America (WNA) from regions that might be considered somewhat analogous to the hard-rock environment of CENA. Two such regions where estimates of κ_0 are available are the Anza region in southern California and the cordillera of southwestern British Columbia, Canada (Table 2).

Table 2 Summary of hard-rock site kappa (κ_0) estimates in WNA.

Source	Mean (sec)	Range (sec)	Comments
Hough et al. [1988]	0.0003	–0.0069–0.0075	Anza KNW; *r* = 0 intercept
Hough et al. [1988]	0.0035	–0.0030–0.0098	Anza PFO; *r* = 0 intercept
Anderson [1991]	0.0019	–	Anza KNW; *r* = 0 intercept
Anderson [1991]	0.0036	–	Anza PFO; *r* = 0 intercept
Silva and Darragh [1995]	0.01	–	KNW & PFO; spectral fitting
Campbell [2009]	0.007	0.0019 – 0.0141	6 Anza sites [Anderson 1991]
Atkinson [1996]	0.011	0.007 – 0.015	WCTN hard-rock sites in B.C.

5.1 ANZA, SOUTHERN CALIFORNIA

Silva et al. [1999] first proposed that the region near Anza might be analogous to the hard-rock environment of CENA. The Anza seismic array is located within the Southern California Batholith, a region of massive granitic rock within the Peninsular Range of southern California. Two of these sites, PFO (Piñon Flat Observatory) and KNW (Keenwild), are located on granitic plutons that are away from any active traces of the San Jacinto fault zone. Deep boreholes drilled near PFO and KNW have respective *S*-wave velocities in excess of 1600 and 1900 m/sec (nearly equal to near-surface velocities of CENA hard-rock sites) at depths below 15 and 20 m and *S*-wave velocities of 2600 and 3000 m/sec (equal to upper-crustal velocities of hard CENA rock) at depths below 50 m [Fletcher et al. 1990]. The more highly weathered rock above depths of 15 and 20 m for PFO-BH and KNW-BH (the BH is used here to distinguish the borehole sites from the nearby array sites of the same designation) has a much lower velocity of approximately 800 m/sec. The array instrument at PFO is located on a pier in a buried vault and the KNW array instrument is located on a concrete pad on an outcrop of "competent" rock. Therefore, the array stations can be considered to be less impacted by the weathered zone and can be used to estimate κ_0 on hard rock for purposes of this study.

Silva and Darragh [1995] estimated a κ_0 of 0.004 sec for KNW and PFO from the $f_{\max}$ values of 38 Hz and 32 Hz estimated by Fletcher et al. [1990] from nearby recordings using the approximate relationship $f_{\max} \approx 1/\pi\kappa$ [Boore 1986]. Using estimates of κ determined from the spectral decay method, Hough et al. [1988] determined κ_0 values of 0.0003 and 0.0035 sec for KNW and PFO, respectively, from the intercept of a linear relationship between κ and distance. Using these same estimates, Anderson [1991] calculated κ_0 values of 0.0019 and 0.0036 sec for these same sites from an interpretation of $\kappa(r)$ in terms of Equation (7). Silva and Darragh [1995] calculated a κ_0 of 0.01 sec for these two sites directly from the recorded spectra using the response spectral fitting approach. Based on data given in Anderson [1991], Campbell [2009] calculated an average κ_0 of 0.007 sec for the six sites of the Anza array where hard rock was encountered at relatively shallow depths. These values are similar to the range of κ_0 values found for hard-rock sites in CENA (Table 1).

As expected, somewhat higher estimates of κ_0 have been found for the borehole sites, which have an upper zone of weathered rock. Fletcher et al. [1990] used vertical seismic profiling (VSP) to estimate a $t*$ of 0.004 sec for KNW-BH and 0.003 sec for PFO-BH over the top 50 m, although they note that their results could be contaminated by near-surface attenuation and interference effects. Aster and Shearer [1991] inverted uphole/downhole spectral ratios in the 2–100 Hz frequency band using generalized reflection/transmission modeling to estimate $Q_{ef} = 9$ over depths of 0–150 m and $Q_{ef} = 27$ over depths of 150–300 m from 20 small earthquakes recorded at KNW-BH. Their comparison of spectral ratios between the surface instrument at KNW and the 300-m deep instrument at KNW-BH yielded $t* = 0.011$ sec in the top 300 m at KNW. This value is over double what others have estimated at KNW using the spectral decay method.

Aster and Shearer [1991] noted that the *P*-wave quality factor was less than or equal to the *S*-wave quality factor in the upper 300 m at KNW-BH, which they interpreted to be an indication that near-surface scattering attenuation is at least as significant as intrinsic attenuation (e.g., Anderson et al. [1965] and Kang and McMechan [1994]). Vernon et al. [1998] came to the same conclusion from an analysis of data recorded by a dense seismic array deployed in the vicinity of PFO-BH, which they attributed to strong scattering of incident body-wave signals into a complex "mishmash" of body-wave and surface-wave modes within the near-surface zone of weathered rock. Dainty [1981] assumed that Q_{in} was independent of frequency, and that Q_{sc} was proportional to frequency for frequencies above 1 Hz; others have followed his example (e.g., Pulli [1984]; Fehler et al. [1988]; and Kang and McMechan [1994]). These assumptions are typically made in efforts to interpret coda-*Q* measurements, for which the variation of coda-*Q* with frequency is thought to reflect scattering effects (e.g., Aki and Chouet [1975] and Morozov

[2008]). If Q_{sc} is indeed proportional to frequency, it will not contribute to the value of κ_0 calculated from the spectral decay method [Anderson and Hough 1984], and the resulting κ_0 will represent only intrinsic attenuation. This could explain the discrepancy between the larger values of t^* and κ_0 found by Aster and Shearer [1991] and Silva and Darragh [1995] at KNW compared to the κ_0 values found by Anderson [1991], who used the spectral decay method proposed by Anderson and Hough [1984]. If this is the case, these latter estimates might be a measure of intrinsic rather than effective attenuation. The same is true for other estimates of site attenuation using the spectral decay method. However, if Morozov [2008; 2009] is correct, then the value of κ_0 derived from the spectral decay method will give a true estimate of effective attenuation.

5.2 SOUTHWESTERN BRITISH COLUMBIA, CANADA

British Columbia, Canada, is another region that can be used to show that the small values of κ_0 reported for CENA hard-rock sites are realistic. Seismometers of the Western Canada Telemetered Network (WCTN) are located on what seismologists call "hard rock," albeit not as hard as CENA hard rock. Atkinson and Cassidy [2000] describe the sites as being older basement rocks in the Lower Mainland area of B.C., consisting mainly of Mesozoic volcanic and sedimentary rocks and granitic intrusions, overlain by Upper Cretaceous and Tertiary strata. The *S*-wave velocity near the surface of these Tertiary bedrock sites is approximately 1.5 km/sec [Hunter et al. 1997]. Limited information is available on the depth distribution of near-surface velocity of these rock sites. It is known from refraction studies (e.g., Spence et al. [1985] and Clowes et al. [1987]) that the velocity increases quite steeply with depth, until values near the midcrustal average of $V_S = 3.7$ km/sec are attained. Based on this limited information, Atkinson and Cassidy [2000] proposed a *S*-wave velocity profile with a steep velocity gradient in the top 200 m from 1.5–3.5 km/sec and a gradual increase in velocity from 3.5–3.7 km/sec below this depth to a depth of 8 km.

Atkinson [1996] used digital ground motion recordings of the WCTN to examine the attenuation and source parameters of earthquakes in southwestern B.C. The database, compiled by Atkinson [1995], was comprised of over 1000 vertical-component Fourier amplitude spectra from earthquakes of magnitude 3 to 7 at distances from 10 to 500 km in southwestern B.C. and northwestern Washington. Atkinson [1996] used only those records within 200 km of well-recorded shallow crustal events in order to limit the uncertainty associated with the anelastic attenuation corrections. This reduced the dataset to 90 records. After correcting the records for geometrical and anelastic attenuation, Atkinson [1996] found that the high-frequency decay of the Fourier amplitude spectra between frequencies of 4 and 14 Hz was consistent with a κ_0 of 0.011 ± 0.002 sec (the range listed in Table 2 represents plus and minus two standard deviations). Although small by WNA standards, this value of κ_0 is about a factor of two larger than that generally found for hard-rock sites in CENA. However, with anelastic attenuation in the shallow crust being significantly greater in B.C. [Atkinson 1995; 2005] than in southeastern Canada and northeastern U.S. [Atkinson 2004], and with B.C. having a slightly softer site profile, it stands to reason that κ_0, which represents attenuation over the top few kilometers of the crust, would also be somewhat larger, further supporting the smaller ($\kappa_0 < 0.01$ sec) values found in CENA.

6 Relationships between Site Kappa and Site Velocity

Another means of estimating κ_0 is by empirically correlating it to the time-averaged *S*-wave velocity in the top 30 m of a site (V_{S30}). Five such relationships are reviewed in this section.

6.1 NORTHERN CALIFORNIA

Silva et al. [1999] developed the following empirical relationship between κ_0 (sec) and V_{S30} (m/sec):

$$\log \kappa_0 = 1.655 - 1.093 \log (V_{S30}) \tag{9}$$

They used strong-motion records at 19 sites with κ_0 ranging from 0.004 to 0.068 sec and V_{S30} ranging from 329 to 1578 m/sec. Estimates of κ_0 were determined using the response spectral fitting approach from point-source inversions of rock recordings from the 1989 Loma Prieta (**M** 6.9) earthquake in northern California [Schneider et al. 1993]. Only those sites with available measured *S*-wave velocity profiles were used in the analysis.

Estimates of κ_0 from Equation (9) or selected values of V_{S30} are summarized in Table 3. Also provided in this table are the NEHRP site classes that correspond to these V_{S30} values [BSSC 2009]. The average values of V_{S30} for site classes B, C, and D are the geometric means of the velocities that define the boundaries of these site classes. The κ_0 values marked with an asterisk in Table 3 are an extrapolation of the equation for NEHRP site classes A, D, D/E, and E.

Table 3 Relationship between site kappa (κ_0) and V_{S30} from Northern California data [Silva et al. 1999].

V_{S30} (m/sec)	κ_0 (sec)	NEHRP Site Class
150	0.19*	E
180	0.16*	D/E
255	0.11*	D
360	0.073	C/D
525	0.048	C
760	0.032	B/C
1070	0.022	B
1500	0.015	A/B
2000	0.011*	A
2500	0.0089*	A
3000	0.0073*	A

* Represents an extrapolation of the model.

6.2 GLOBAL ACTIVE AND STABLE TECTONIC REGIMES

Chandler et al. [2006] developed an empirical relationship that can be used to estimate κ_0. This relationship was developed from published values of Q_0, the quality factor at a frequency of 1 Hz, published and estimated values of κ_0, and regional velocity models obtained from the Global Crustal Model CRUST2.0 [IGPP 2001]. The basis for the model is a modified version of an equation proposed by Boore [2003]:

$$\kappa_0 = R_{uc} / (Q_{uc} V_{uc}) \tag{10}$$

where R_{uc} is the thickness of the upper crust (assumed to be 4 km), and Q_{uc} is the quality factor of the upper crust. V_{uc} is the time-averaged *S*-wave velocity of the upper crust, which is calculated from the equations:

$$V_{uc} = \frac{R_{uc}}{\sum_i dz_i / V_{Si}} \quad \text{or} \quad \frac{R_{uc}}{\int_0^{R_{uc}} dz / V_S} \tag{11}$$

where i is the layer number, dz_i is the thickness of the layer, and V_{Si} is the estimated *S*-wave velocity of the layer from CRUST2.0.

Chandler et al. [2006] compiled a consistent set of published values of κ_0 ranging from 0.011 to 0.07 sec and a set of published values of Q_0 ranging from 100 to 400 for seven regions in Italy, central Europe, British Columbia, WNA, and California. For each of these regions, they estimated V_{uc} from CRUST2.0 and used this estimate of upper crustal velocity along with κ_0 and the assumption that $R_{uc} = 4$ km to calculate Q_{uc} from Equation (10). This analysis showed that the ratio of Q_{uc} to Q_0 was relatively constant at $Q_{uc}/Q_0 \approx 0.2$. In a second phase of the study, Chandler et al. [2006] compiled an additional database of 22 published values of Q_0, bringing the total number to 29 with values ranging from 47 to 1000. These values represented 17 regions with generic rock profiles located in both active and stable tectonic regimes worldwide. Regional values of V_{uc} were obtained from CRUST2.0, and Q_{uc} was estimated from Q_0 using the previously derived ratio between Q_{uc} and Q_0. Using these values of V_{uc} and Q_{uc}, and assuming $R_{uc} = 4$ km, they estimated values of κ_0 from Equation (10), resulting in a total of 33 published and estimated values of κ_0 ranging from 0 to 0.081 sec. They used this database to develop the following relationship between κ_0 (sec) and upper crustal velocity (km/sec):

$$\kappa_0 = 0.145 - 0.12 \ln V_{uv} \tag{12}$$

which is considered to be valid for $1.6 \le V_{uc} \le 3.35$ km/sec. The upper limit of V_{uc} is constrained at the value at which this relationship predicts $\kappa_0 = 0$.

In order to make Equation (12) of greater use to engineers, Chandler et al. [2006] used the parametric modeling approach of Chandler et al. [2005] together with the regional crustal profiles used to estimate V_{uc} to develop representative shallow crustal velocity profiles, or what Chandler et al. [2005] call the upper sedimentary crustal layers, for each region. In this way, Chandler et al. [2006] estimated the *S*-wave velocity at a depth of 0.03 km (30 m) within the profile, which they refer to as $V_{s,0.03}$. Using these estimates of $V_{s,0.03}$, they developed the following relationship between κ_0 (sec) and $V_{s,0.03}$ (km/sec):

$$\kappa_0 = \left(0.057/V_{s,0.03}^{0.8}\right) - 0.02 \tag{13}$$

which is considered to be valid for $0.5 \le V_{s,0.03} \le 3.0$ km/sec. $V_{s,0.03}$ should not be confused with V_{S30}, the average *S*-wave velocity in the top 30 m. Using these same shallow crustal profiles, Chandler et al. [2006] found that $V_{S30} \approx 0.75\, V_{s,0.03}$ for the upper sedimentary crustal layer, which extends to depths ranging from 0 in glaciated regions to several kilometers in deep basins. The relationship between $V_{s,0.03}$ and V_{S30} used in the current study is modified to become a function of V_{S30} as follows: $V_{s,0.03} = V_{S30}/0.75$ for $V_{S30} \le 760$ m/sec and $V_{s,0.03} = V_{S30}$ for $V_{S30} \ge 3000$ m/sec, with a linear transition in the divisor for intermediate velocities. This transition is intended to account for the steepening of the near-surface velocity gradient in typical rock profiles representing NEHRP site classes A and B. These substitutions and modifications result in the following relationship between κ_0 (sec) and V_{S30} (m/sec):

$$\kappa_0 = 14.318\left(V_{S30}/c\right)^{-0.8} - 0.02 \tag{14}$$

where

$$c = \begin{cases} 0.75; & V_{S30} \leq 760 \\ 0.75 + 0.25\left(1 - \left[(3000 - V_{S30})/2240\right]\right); & 760 < V_{S30} < 3000 \\ 1.0; & V_{S30} \geq 3000 \end{cases} \quad (15)$$

Estimates of κ_0 from Equations (14) and (15) are summarized in Table 4 for the same values of V_{S30} that are listed in Table 3. Also provided in these tables are the NEHRP site classes that correspond to these V_{S30} values [BSSC 2009]. The average values of V_{S30} for site classes B, C, and D are the geometric means of the velocities that define the boundaries of these three site classes.

Table 4 Relationship between site kappa (κ_0) and V_{S30} from global data [Chandler et al. 2006].

V_{S30} (m/sec)	$V_{S,0.03}$ (m/sec)	κ_0 (sec)	NEHRP Site Class
150	200	0.19*	E
180	240	0.16*	D/E
255	340	0.12*	D
360	480	0.083	C/D
525	700	0.056	C
760	1010	0.036	B/C
1070	1360	0.025	B
1500	1800	0.016	A/B
2000	2250	0.0098	A
2500	2650	0.0062	A
3000	3000	0.0037	A

* Represents an extrapolation of the model

6.3 FRANCE

Drouet et al. [2010] inverted the Fourier amplitude spectra of hundreds of records from the French strong-motion network to jointly determine source, path, and site properties. The records came from magnitude 3 to 5 earthquakes in three regions of France: the Alps (72 events), the Rhine Graben (23 events), and the Pyrenees (66 events). By fitting the attenuation operator $\exp(-\pi\kappa_0 f)$ to the high-frequency part of the site transfer function, there were a sufficient number of records to determine κ_0 at 76 of these recording sites. By comparing the ratio of the estimated site transfer functions with those derived from generic site profiles of varying values of V_{S30}, they were able to estimate V_{S30} at 21 rock sites with an accuracy of about 500 m/sec.

Although noting a trend of decreasing κ_0 with V_{S30}, they chose not to fit an equation to this trend because of the large uncertainty associated with the estimation of both κ_0 and site velocity. They attributed this large uncertainty in part to the effects of the deeper structure (e.g., Campbell [2009]).

Douglas et al. [2010] determined κ_0 at nine of the same recording sites using the method of Anderson and Hough [1984]. κ_0 was estimated as the intercept of a linear relationship between κ and distance for three regions in France using a database similar to that of Drouet et al. [2010]. Although there is a clear relationship between the κ_0 values determined by both methods, those of Douglas et al. [2010] are generally smaller, in some cases by over 50%. Drouet et al. [2010] noted that their results are less likely to be impacted by source effects because of the joint inversion method that they used. Drouet et al. [2010] also compared their estimates with Equation (9) and generally found them to be smaller for a given value of V_{S30}. It is interesting to note that Douglas et al. [2010] determined average values of κ_0 for soil sites $(\kappa_0 = 0.0270)$ and rock sites ($\kappa_0 = 0.0207$ sec), and noted that their estimate for rock sites is intermediate to that for soft-rock sites in WNA and hard-rock sites in CENA, consistent with regional estimates of Q [Campillo et al. 1985].

6.4 SWITZERLAND

Edwards et al. [2011] used two methods to estimate κ_0 in Switzerland. In the first method, they performed a broadband inversion of the Fourier amplitude spectra of over 18,000 individual horizontal components from the Swiss seismological network to jointly determine source and attenuation properties using the generic rock Swiss amplification function of Poggi et al. [2011]. The records came from 720 magnitude 2 to 5 earthquakes in Switzerland and the immediate surrounding area. Path attenuation was represented by the t^* parameter defined in Equation (4), which was separated into a crustal quality factor (Q_0) and a site attenuation parameter (κ_0) using the linear distance-dependent relationship of Anderson and Hough [1984]. The slope of this relationship can be interpreted as $(Q_0\beta_0)^{-1}$ assuming a simple crustal model of a layer over a half-space. Assuming $\beta_0 = 3.5$ km/sec, the average and standard deviation estimates of crustal and site attenuation were found to be $Q_0 = 1216^{+149}_{-33}$ and $\kappa_0 = 0.0157 \pm 0.0026$ sec, valid to distances of 220 km. This value of κ_0 can be compared to those of Bay et al. [2003; 2005], who found average values of κ_0 of 0.015 and 0.0125 sec, respectively, for Swiss sites classified as NEHRP A and B (i.e., $V_{S30} > 760$ m/sec), to that of Morasca et al. [2006], who found an average κ_0 of 0.012 sec for rock sites in the western Alps, and to that of Douglas et al. [2010], who found an average κ_0 of 0.0207 sec for rock sites in France. A simultaneous fit of crustal attenuation and κ_0 using a matrix inversion method resulted in alternative values of $Q_0 = 1194$ and $\kappa_0 = 0.020$ sec. Restricting the inversion to only high-quality records (24% fewer records) resulted in a Q_0 of 1317, well within the one standard deviation range of the value found for the entire dataset.

The robustness of the simultaneous inversion method was tested by applying the method of Anderson and Hough [1984] directly to the records. In order to ensure that the Fourier amplitude spectra above 10 Hz were above the source corner frequency, only earthquakes with $M_W \geq 3.5$ were used, resulting in 823 individual horizontal records from 47 events. Q_0 was constrained to a frequency-independent value of 1200, as the quantity of data remaining were too few to robustly define both crustal attenuation and κ_0. A comparison of the κ_0 values determined by the Anderson and Hough [1984] method with those determined by the simultaneous fit method indicated that the latter method did not introduce any systematic bias or trade-off.

Using the individual values of κ_0 (sec) derived from the simultaneous fit method and the values of V_{S30} (m/sec) determined by Fäh et al. [2009], Edwards et al. [2011] determined two relationships for κ_0, one in terms of $\log(\kappa_0)$:

$$\log(\kappa_0) = -1.49 - 0.000278\,V_{S30} \tag{16}$$

and a second in terms of κ_0:

$$\kappa_0 = 0.0289 - 0.00000838\,V_{S30} \tag{17}$$

It was difficult for the authors to distinguish which equation was better due to the large scatter in the data, as indicated by the relatively low R^2 value of 0.381 between κ_0 and V_{S30}.

Edwards [2012] revised the κ_0 relationships of Edwards et al. [2011] in order to correct an error in the value of V_{S30} that they had used to characterize the Swiss seismological stations. They had mistakenly used V_{S40}, or the time-averaged value of *S*-wave velocity in the top 40 m of the site profile. Edwards also used this opportunity to add a log-log relationship to the Lin-Lin and log-lin equations of Edwards et al. [2011]. The revised equations, using all of the Swiss seismological stations for which a V_{S30} was estimated by Fäh et al. [2009], are given by:

$$\log(\kappa_0) = -1.51 - 0.00031\,V_{S30} \tag{18}$$

$$\log(\kappa_0) = 0.0854 - 0.653\log(V_{S30}) \tag{19}$$

$$\kappa_0 = 0.0274 - 0.0000087\,V_{S30} \tag{20}$$

where κ_0 and V_{S30} have units of sec and m/sec, respectively. Estimates of κ_0 from Equations (18) to (20) are summarized in Table 5for the same values of V_{S30} that are listed in Table 3. Also provided in these tables are the NEHRP site classes that correspond to these V_{S30} values [BSSC

2009]. The average values of V_{S30} for site classes B, C, and D are the geometric means of the velocities that define the boundaries of these three site classes.

Table 5 Relationship between site kappa (κ_0) and V_{S30} from Swiss data [Edwards et al. 2011; Edwards 2012].

V_{S30} (m/sec)	κ_0 (sec)			NEHRP Site Class
	E12a	E12b	E12c	
150	0.028*	0.046*	0.026*	E
180	0.027*	0.041*	0.026*	D/E
255	0.026*	0.033*	0.025*	D
360	0.024	0.026	0.024	C/D
525	0.021	0.020	0.023	C
760	0.018	0.016	0.021	B/C
1070	0.014	0.013	0.018	B
1500	0.011	0.010	0.014	A/B
2000	0.0074**	0.0085**	0.010**	A
2500	0.0052**	0.0074**	0.0057**	A
3000	0.0036**	0.0065**	0.0013**	A

Abbreviations are defined as follows: E12a, Edwards [2012] Log-Lin relationship; E12b, Edwards [2012] Log-Log relationship; E12c, Edwards [2012] Lin-Lin relationship.

* Represents an extrapolation of the model.

** There is only one value of V_{S30} for $V_{S30} > 1800$ m/sec.

6.5 JAPAN, CALIFORNIA, AND TAIWAN

Van Houtte et al. [2011] estimated κ_0 for (1) 4554 surface and downhole KiK-net recordings from 267 magnitude 4 to 7.2 shallow crustal earthquakes in Japan and (2) 190 Next Generation Attenuation (NGA) recordings [Chiou et al. 2008] from 27 magnitude 4.8 to 7.7 shallow crustal earthquakes in California and Taiwan. In order to select stations located on stiff soil or rock, they only used stations with measured V_{S30} at the surface greater than 500 m/sec. κ values were determined using the method of Anderson and Hough [1984], estimating κ_0 as the zero-distance intercept of the curve determined by independently fitting a linear relationship between κ and distance for each region, which they interpret as regional differences in regional attenuation properties (i.e., *Q*). The distance term for the Japanese recordings was estimated from only downhole recordings to avoid site amplifications that could bias the distance term.

Because of the large number of Japanese recordings, Van Houtte et al. [2011] were able to investigate the dependence of κ on (1) the site, (2) the source, and (3) the site and source. The distance dependence was also investigated in each of these cases (six cases in all). The lowest variance was found for the model in which site (κ_0), source, and distance terms were included, although an F-Test indicated that the most significant model was that in which only the site and distance terms were included. Unlike many studies that determine κ_0 by inversion of the data for source, path, and site-amplification effects, Van Houtte et al. [2011] found that all of the estimated values of κ were positive, except for a few downhole values that had values close to zero. This was also the case for the California and Taiwan data. However, they did find that the surface and downhole values of κ_0 were correlated with an average shift of 0.015 sec for the downhole sites (mean of 0.017 sec and standard deviation of 0.010 sec) compared to the surface sites (mean of 0.033 sec and standard deviation of 0.012 sec). Oth et al. [2011] found similar results with means of 0.015 sec for the downhole recordings and 0.029 sec for the surface recordings, and a standard deviation of 0.08 sec for both.

A regression of all data by Van Houtte et al. [2011] resulted in the following relationship between κ_0 (sec) and V_{S30} (m/sec):

$$\ln(\kappa_0) = 3.490 - 1.062\ln(V_{S30}) \tag{21}$$

with a correlation coefficient of 0.39 and a standard error of 0.55. The κ_0 estimates that Van Houtte et al. [2011] obtained from the Japanese and NGA data are compared to the κ_0 estimates of Silva et al. [1999], Chandler et al. [2006], Douglas et al. [2010], Drouet et al. [2010], and Edwards et al. [2011] in Part A of Figure 3; their $\kappa_0 - V_{S30}$ relationship is compared to the relationships of Silva et al. [1999] and Chandler et al [2006] in Part B of Figure 3. This figure also shows the large amount of scatter in the κ_0 estimates as well as the small amount of data for sites with $V_{S30} > 2000$ m/sec of primary concern in this study. Estimates of κ_0 from Equation (21) are summarized in Table 6for the same values of V_{S30} that are listed in Table 3. Also provided in this table are the NEHRP site classes that correspond to these V_{S30} values [BSSC 2009]. The average values of V_{S30} for site classes B, C, and D are the geometric means of the velocities that define the boundaries of these three site classes.

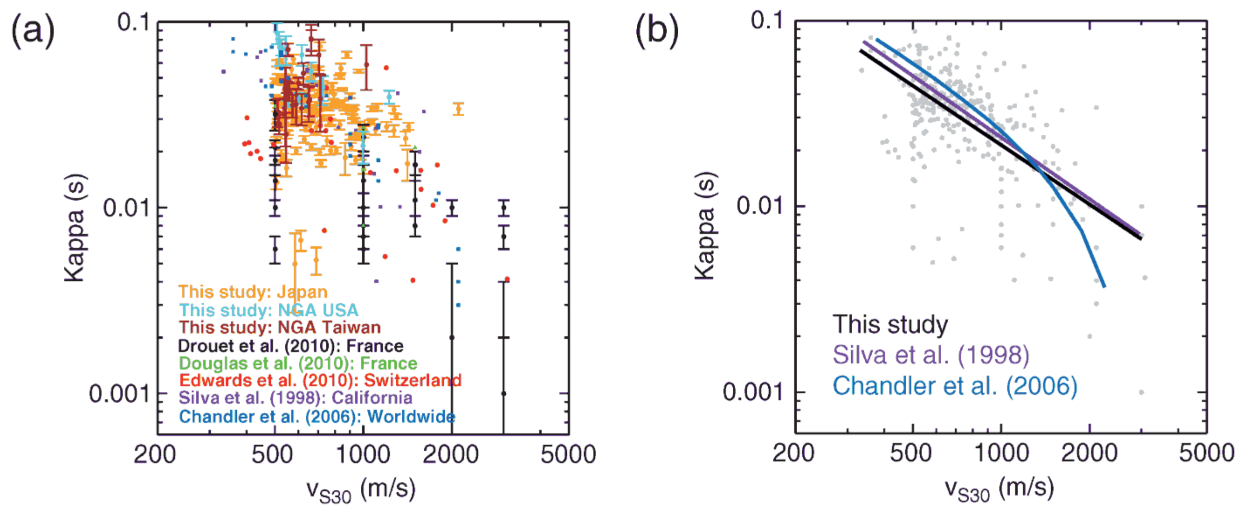

Figure 3 (a) Compilation of $\kappa_0 - V_{S30}$ data from various studies as indicated in the legend and in the list of references in the present report; and (b) $\kappa_0 - V_{S30}$ data from Van Houtte et al. [2011] compared to three empirically derived relationships. In both plots, this study refers to the study of Van Houtte et al. [2011]. Source: Van Houtte et al. [2011] Figure 10.

Table 6 Relationship between site kappa (κ_0) and V_{S30} from Japanese and NGA California and Taiwan data [Van Houtte et al. 2011].

V_{S30} (m/sec)	κ_0 (sec)	NEHRP Site Class
150	0.16*	E
180	0.13*	D/E
255	0.091*	D
360	0.063	C/D
525	0.042	C
760	0.029	B/C
1070	0.020	B
1500	0.014	A/B
2000	0.010	A
2500	0.0081	A
3000	0.0067	A

* Represents an extrapolation of the model.

6.6 DISCUSSION

Table 7 summarizes κ_0 estimates from the $\kappa_0 - V_{S30}$ relationships of Silva et al. [1999] [Sea99] for northern California, Chandler et al. [2006] [Cea06] for global active and stable tectonic regimes, Edwards et al. [2011] as modified by Edwards [2012] [E12a,b,c] for Switzerland, and Van Houtte et al. [2011] [Vea11] for Japan, California, and Taiwan. Except for Switzerland, all of the equations give similar estimates of κ_0 for $V_{S30} < 1500$ m/sec, after which they begin to diverge due to their different databases and functional forms, and greater uncertainty. The Switzerland equations systematically predict smaller estimates in this velocity range for reasons that are not known at this time. One possible reason is that Edwards et al. [2011] and Edwards [2012] allowed negative values of κ_0 in their inversions, thus reducing the average value for each station compared to an analysis for which all values of κ_0 are found or constrained to be greater than zero. However, the Swiss estimates become more similar to those from the other relationships at higher values of V_{S30}.

Table 7 Summary of site kappa estimates from $\kappa_0 - V_{S30}$ relationships developed from various studies.

V_{S30} (m/sec)	κ_0 (sec)						NEHRP Site Class
	Sea99	Cea06	E12a	E12b	E12c	Vea11	
150	0.19*	0.19*	0.028*	0.046*	0.026*	0.16*	E
180	0.16*	0.16*	0.027*	0.041*	0.026*	0.13*	D/E
255	0.11*	0.12*	0.026*	0.033*	0.025*	0.091*	D
360	0.073	0.083	0.024	0.026	0.024	0.063	C/D
525	0.048	0.056	0.021	0.020	0.023	0.042	C
760	0.032	0.036	0.018	0.016	0.021	0.029	B/C
1070	0.022	0.025	0.014	0.013	0.018	0.020	B
1500	0.015	0.016	0.011	0.010	0.014	0.014	A/B
2000	0.011*	0.0098	0.0074*	0.0085*	0.010*	0.010	A
2500	0.0089*	0.0062	0.0052*	0.0074*	0.0057*	0.0081	A
3000	0.0073*	0.0037	0.0036*	0.0065*	0.0013*	0.0067	A

Note: Abbreviations are defined as follows: Sea99, Silva et al. [1999]; Cea06, Chandler et al. [2006]; E12a, Edwards [2012] Log-Lin relationship; E12b, Edwards [2012] Log-Log relationship; E12c, Edwards [2012] Lin-Lin relationship; Vea11, Van Houtte et al. [2011]

* Represents an extrapolation of the model

For hard-rock *S*-wave velocities of $V_{S30} > 2000$ m/sec that are of primary interest in this study, the estimates of κ_0 from Cea06, which range from 0.004–0.01 sec and include data from stable continental regions, are consistent with those reported in Table 1 for CENA hard-rock sites (0.004–0.008 sec if the problematic Monticello estimates are excluded). In fact, all of the relationships provide estimates of κ_0 for $V_{S30} > 2000$ m/sec that are comparable to the values of given in Table 1, whether or not they explicitly include data from stable continental regions or, for that matter, from hard-rock sites in general. For *S*-wave velocities of $V_{S30} > 1500$ m/sec, the estimates of κ_0 from the $\kappa_0 - V_{S30}$ relationships are found to range from 0.004–0.016 sec, which are consistent with those reported in Table 2 for British Columbia hard-rock sites (0.007–0.015 sec) with similar near-surface velocities. The E12c Lin-Lin relationship is excluded from this comparison because of its extreme curvature at large values of V_{S30}.

Although not directly relevant to the estimation of κ_0 for hard-rock sites, it is interesting to compare estimates of κ_0 from the $\kappa_0 - V_{S30}$ relationships listed in Table 7 with those reported for soft rock more typical of the WUS, herein defined as sites with $V_{S30} = 525 - 760$ m/sec (the upper range of NEHRP site class C). This range encompasses the generic soft-rock site profile of Boore and Joyner [1997], which has an empirically derived V_{S30} of 620 m/sec. For this range of V_{S30} values, Sea99 predicts $\kappa_0 = 0.032 - 0.048$ sec (0.039 sec median), Cea06 predicts $\kappa_0 = 0.036 - 0.056$ sec (0.045 sec median), and Vea11 predicts $\kappa_0 = 0.029 - 0.042$ sec (0.036 sec median). These values are within the range of κ_0 values that have been reported for generic soft-rock sites in WNA [Anderson and Hough 1984; Silva and Darragh 1995; Boore and Joyner 1997; and Silva et al. 1999]. They are also consistent with the range (0.037–0.044 sec) found for generic rock sites by inverting the NGA GMPEs using the point-source stochastic simulation method (W. Silva, personal communication). This consistency confirms the general reliability of these equations.

Anderson et al. [1996] performed theoretical wave-propagation analyses for typical *S*-wave velocity profiles of the upper 5 km of the crust to determine if upper-crustal estimates of κ_0 could be related to V_{S30}. The *S*-wave velocity and quality factor at the base of the profile were assumed to be $V_S = 3640$ m/sec and $Q = 1000$, respectively. The *S*-wave velocity and quality factor in the 30-m-thick surface layer were varied with typical values of $V_{S30} = 180$ m/sec and $Q = 15$ (representing a NEHRP D/E site class), $V_{S30} = 365$ m/sec and $Q = 25$ (representing a NEHRP C/D site class), $V_{S30} = 760$ m/sec and $Q = 35$ (representing a NEHRP B/C site class), and $V_{S30} = 1500$ m/sec and $Q = 50$ (representing a NEHRP A/B site class). Intervening layers were assumed to have properties that were intermediate to these. For site profiles in which the *S*-wave velocity and the quality factor monotonically increases with depth, they discovered that high-frequency amplification is controlled by two nearly equally important components: (1) the surface geology, represented by V_{S30}, and (2) the cumulative damping over the entire 5 km thickness of the profile, represented by the attenuation parameter $t*$. Although their results are given in terms of $t*$, the authors show that $t*$ is virtually identical to κ_0 for the assumptions used in the model (particularly the assumption that *Q* is independent of frequency). They found a relatively strong relationship between V_{S30} and t^* (or κ_0), as shown in Figure 4, where site amplification is defined in terms of a "stratified medium index" (SMI); this SMI is defined as the time integral of the square of acceleration at the surface of the site profile divided by four times the time integral of the square of the acceleration at the base of the site profile. This led them to propose the preliminary relationship between κ_0 and V_{S30} given in Table 8. The values in this table confirm the empirical trends summarized in Table 7; however, they are generally smaller at small velocities and larger at large velocities, indicating a different velocity and attenuation profile than implied by the empirical data.

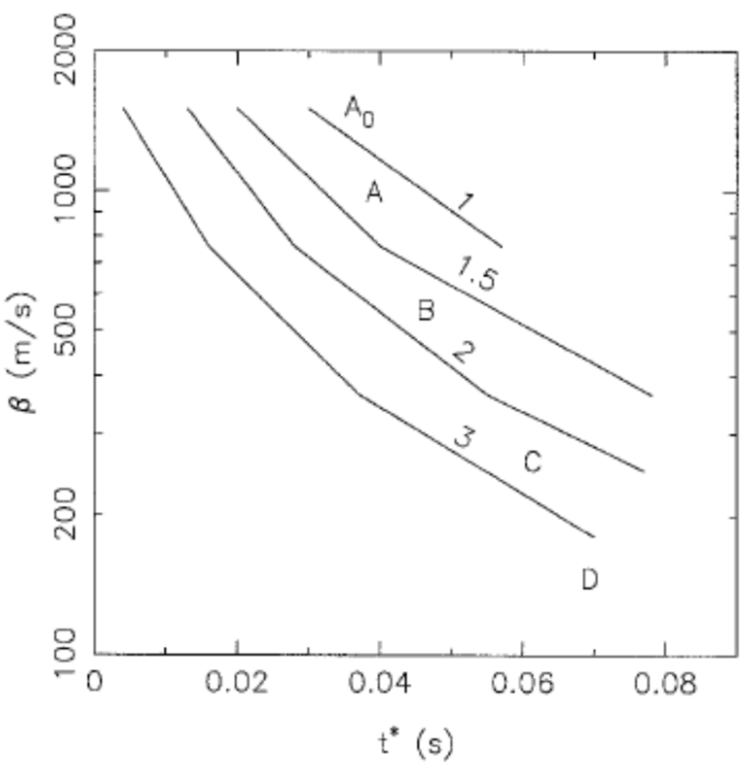

Figure 4 **Relationship between V_{S30} (denoted β) and κ_0 (denoted t^*) from synthetic seismograms for 5-km-deep upper crustal profiles with monotonically increasing *S*-wave velocity (Figure 11 from Anderson et al. [1996]). The letters represent the site class designations of Boore et al. [1993], which are related to the NEHRP site class designations given in Table 7. The numbers designate upper crustal amplification given in terms of the simplified medium index (SMI) described in the text.**

Table 8 Relationship between site kappa (κ_0) and (V_{S30}) from synthetic seismograms for a typical upper crustal site profile in WNA [Anderson et al. 1996].

V_{S30} (m/sec)	κ_0 (sec)	Boore Site Class	NEHRP Site Class
180	0.070	C – D	D/E
360	0.055	B – C	C/D
760	0.040	A – B	B/C
1500	0.035	A_0 – A	A/B

7 Interpretation of Results

7.1 MEAN AND MEDIAN SITE KAPPA

The mean and median (geometric mean) of the 10 estimates of κ_0 on hard-rock sites in CENA listed in Table 1 are 0.0062 and 0.0058 sec, respectively, when the Monticello Reservoir recordings are included, and 0.0057 and 0.0053 sec, respectively, when they are not. These values are virtually identical to the 0.006 sec median value proposed by EPRI [1993] to represent the upper crustal attenuation of hard-rock sites in CENA. It is also consistent with several other assessments, including:

1. the mean (0.0065 sec) and median (0.0062 sec) values obtained for the 14 hard-rock recordings (excluding the Monticello Reservoir recordings) reported by Silva and Darragh [1995];
2. the 0.005-sec value (i.e., the midpoint of the range of κ_0 values found by Atkinson and Boore [2006] for hard-rock sites in the cratonic region of CENA) that was used by Campbell [2009] to represent the hard-rock component of site attenuation in his estimates of κ_0 for sedimentary sites in CENA;
3. the mean (0.0052 sec) and range (0–0.01 sec) for the average values determined for very hard granite batholith sites at Anza, California (Table 2);
4. the mean 0.006-sec value determined from a preliminary stochastic simulation model of ground motion recordings in southwestern Australia [Allen 2012];
5. the range (0.001–0.011 sec) estimated from six prediction equations between κ_0 and V_{S30}, assuming that CENA hard rock can be represented by sites with $V_{S30} = 2000 - 3000$ m/sec (Table 7); and
6. the estimated value of 0.006 sec for an assumed shear-wave Q of at least 1600 for $f > 10$ Hz based on regional studies in the Appalachians, a basement shear-wave velocity of 3.45 km/sec, and distances within 30 km of the source [Chapman et al. 2003].

Excluding the Lin-Lin relationship of Edwards [2012], whose prediction rapidly approaches zero, the five other $\kappa_0 - V_{S30}$ relationships predict a mean κ_0 of 0.0056 sec (range of 0.0036–

0.0073 sec) for a V_{S30} of 3000 m/sec, which is the reference-rock velocity for CENA recommended for the NGA-East Project by the Geotechnical Working Group [Hashash et al. 2014a,b].

7.2 UNCERTAINTY IN SITE KAPPA

The arithmetic and natural log standard deviations of the 10 estimates of κ_0 on hard-rock sites in CENA listed in Table 1 are 0.0022 sec and 0.45, respectively, when the Monticello Reservoir recordings are included, and 0.0022 sec and 0.47, respectively, when they are not. Assuming a normal distribution, the arithmetic standard deviations correspond to a coefficient of variation (COV) of 0.36, when the Monticello Reservoir recordings are included, and 0.38 when they are not, based on the arithmetic mean values given in the previous section. Assuming a lognormal distribution, the natural log standard deviations result in a COV of 0.47, when the Monticello Reservoir recordings are included, and 0.50 when they are not. There are too few data to reliably determine what probability distribution is appropriate for characterizing the uncertainty in κ_0. Since Fourier spectral amplitude is related to κ_0 through the exponential attenuation operator given by Equation (5), and since Fourier amplitudes are typically assumed to be lognormally distributed (e.g., Atkinson and Silva [1997]), one might argue that κ_0 should be normally distributed. However, the theoretical limitation that $\kappa_0 \geq 0$ argues for a uniform, truncated normal, lognormal, or other probability distribution that does not allow negative values. Most investigators have treated κ_0 as being either uniformly or lognormally distributed. EPRI [1993] used three equally weighted values of κ_0 (0.003, 0.006, and 0.012 sec) to model aleatory uncertainty in this parameter in its development of a CENA GMPE using the point-source stochastic simulation method. This range represents a factor of two around EPRI's median value of 0.006 sec; therefore, it is not strictly a uniform distribution. Atkinson and Boore [2006] used a uniform distribution of 0.005 ± 0.003 sec to model the aleatory uncertainty of κ_0 in their development of a CENA GMPE using the finite-source stochastic simulation method.

EPRI [1993] used a lognormal distribution with a median κ_0 of 0.006 sec and a standard deviation of $\sigma_{\ln \kappa_0} = 0.40$ to study the effect of the uncertainty in κ_0 on the prediction of spectral accelerations using the point-source stochastic simulation method. They attribute this standard deviation to the range of values estimated from the regression of 20 strong ground motion records at northern California rock sites that recorded the 1989 Loma Prieta (**M** 6.9) earthquake [Schneider et al. 1993]. Silva and Darragh [1995] assumed a lognormal distribution for κ_0 in estimating a median κ_0 of 0.007 sec and a standard deviation of $\sigma_{\ln \kappa_0} = 0.42$ for 16 hard-rock sites in CENA (including the two problematic recordings at Monticello Reservoir). Removing the Monticello recordings results in a smaller median κ_0 of 0.0062 sec and a smaller standard deviation of $\sigma_{\ln \kappa_0} = 0.34$. Assuming a normal distribution results in a mean and standard deviation of 0.0076 and 0.0033 sec, including the Monticello Reservoir recordings, and 0.0066 and 0.0020 sec without them. The coefficient of variations (COVs) of these latter statistics are 0.43 and 0.30, respectively.

Silva et al. [2002] used a median κ_0 of 0.006 sec and a standard deviation of $\sigma_{\ln\kappa_0} = 0.3$ to characterize aleatory and epistemic uncertainty in κ_0 in their development of a CENA hard-rock GMPE using the point-source stochastic simulation method. They attribute this standard deviation to the variability determined from the same 20 strong ground motion records at northern California rock sites that recorded the Loma Prieta earthquake [Schneider et al. 1993] that were used by EPRI [1993] to justify its 0.40 value. They admit that this variability seems a little low to characterize both aleatory and epistemic uncertainty, but claim that there is additional uncertainty in the analysis by assuming a constant soft-rock κ_0 of 0.03 sec in the validation exercises that they used to develop the stochastic simulation model [Silva et al. 1997; Appendix A of Silva et al. 2002].

Because of the apparent contradiction in the standard deviations of κ_0 that EPRI [1993] and Silva et al. [2002] attributed to the analysis of the 20 rock recordings from the Loma Prieta earthquake [Schneider et al. 1993], it was decided that an independent statistical analysis of these values should be performed. Schneider et al. [1993] reported values that were derived from three different models based on a version of the finite-fault stochastic simulation method that uses theoretical rather than empirical Green's functions [Silva et al. 1990]. Model 0 assumed typical values for the source and path parameters, and fit the κ_0 values by eye. Models 1 and 2 inverted the strong ground motion records for the source, path, and site parameters; the difference being that Model 1 used r^{-1} geometrical attenuation and Model 2 used a geometrical attenuation relationship that included critical reflections off the Moho [Ou and Herrmann 1990]. The resulting κ_0 values are listed in Table 9, and a summary of the statistics of these values is given in Table 10. The statistics were derived assuming uniform, normal, and lognormal probability distributions. Assuming a normal distribution, Models 0, 1, and 2 result in standard deviations of 0.027, 0.017, and 0.016 sec, respectively. Assuming a lognormal distribution, these three models result in natural log standard deviations of 0.42, 0.65, and 0.54, respectively, which are considerably larger than the 0.3 value used by Silva et al. [2002] attributed to the same dataset. W. Silva (personal communication) said that Silva et al. [2002] obtained a smaller value by weighting the κ_0 values from Models 1 and 2 by the inverse of their standard errors from the inversion, which heavily weighted the value obtained from the Corralitos (COR) recording station and down-weighted the values from the other 19 sites. The value used in the EPRI [1993] sensitivity study is very similar to the standard deviation obtained for Model 0.

Table 9 Estimates of site kappa (κ_0) from Loma-Prieta rock recordings [Schneider et al. 1993].

Station	κ_0 (sec)		
	Model 0	Model 1	Model 2
COR	0.055	0.064	0.074
GL1	0.025	0.033	0.039
UCS	0.040	0.027	0.032
GL6	0.050	0.054	0.055
SLAC	0.060	0.054	0.053
RDC	0.120	0.057	0.052
SAS	0.100	0.070	0.064
A07	0.100	0.048	0.040
A10	0.100	0.068	0.060
MON	0.060	0.038	0.029
BEL	0.080	0.055	0.047
A2E	0.040	0.045	0.046
SSP	0.040	0.015	0.014
SFD	0.040	0.026	0.029
PHS	0.050	0.027	0.031
SFR	0.040	0.004	0.007
YBI	0.080	0.047	0.050
SFH	0.080	0.041	0.044
SFT	0.040	0.034	0.036
SFC	0.080	0.035	0.037

Table 10 **Statistics of site kappa (κ_0) estimates from the Loma-Prieta earthquake rock recordings in Table 9.**

Distribution		Mean or Median	Standard Deviation	COV	Minimum or -2σ	Maximum or $+2\sigma$
Lognormal	Model 0	0.059	0.424	0.444	0.025	0.137
	Model 1	0.037	0.649	0.724	0.010	0.134
	Model 2	0.038	0.540	0.582	0.013	0.111
Normal	Model 0	0.064	0.027	0.422	0.011	0.117
	Model 1	0.042	0.017	0.405	0.007	0.077
	Model 2	0.042	0.016	0.381	0.010	0.074
Uniform	Model 0	0.073	–	–	0.025	0.120
	Model 1	0.039	–	–	0.004	0.070
	Model 2	0.041	–	–	0.007	0.074

8 Recommended Reference-Rock Site Kappa for CENA

8.1 RECOMMENDED MEDIAN VALUE OF REFERENCE-ROCK SITE KAPPA

Based on the results of this study, and careful deliberation of the NGA-East Geotechnical Working Group (GWG), it is recommended that the reference-rock site kappa ($\kappa_{0,ref}$) for a reference-rock *S*-wave velocity ($V_{s,ref}$) in CENA, defined as having a central estimate of 3000 m/sec and range of 2700–3300 m/sec [Hashash et al. 2014a,b], should be represented by a lognormal distribution with a median value ($\bar{\kappa}_{0,ref}$) of 0.006 sec (Table 11). A lognormal distribution for $\kappa_{0,ref}$ was chosen because: (1) it has been used to represent the distribution of κ_0 in several studies and, therefore, has precedence in the literature; and (2) it was decided that the distribution should not allow for the unphysical prediction of negative values. The selection of the median value was straightforward, based on the values presented in this report. However, selecting a value for aleatory uncertainty and, especially, for epistemic uncertainty required more consideration, as summarized below.

Table 11 Recommended distribution of reference-rock site kappa (κ_0) in CENA.

Distribution Parameter*	Value
Type of Distribution	Lognormal
Median, $\kappa_{0,ref}$ (sec)	0.006
Aleatory Standard Deviation, $\phi_{\ln\kappa_{0,ref}}$ (sec)	0.43
Epistemic Standard Deviation, $\varepsilon_{\ln\kappa_{0,ref}}$ (sec)	
Excluding source, path, and site uncertainty	0.12
Including source, path, and site uncertainty	0.20
Total Standard Deviation, $\sigma_{\ln\kappa_{0,ref}} = \sqrt{\phi^2_{\ln\kappa_{0,ref}} + \varepsilon^2_{\ln\kappa_{0,ref}}}$	
Excluding source, path, and site uncertainty	0.45
Including source, path, and site uncertainty	0.47
Coefficient of Variation $\left(\mathrm{COV} = \sqrt{\exp(\sigma^2) - 1}\right)$	
Aleatory variability	0.45
Epistemic uncertainty	
Excluding source, path, and site uncertainty	0.47
Including source, path, and site uncertainty	0.50
95th Confidence Internal; $\pm 2\sigma$ Range (sec)	
Excluding source, path, and site uncertainty	0.0024 – 0.0148
Including source, path, and site uncertainty	0.0023 – 0.0154

* Assumes a reference CENA hard-rock site with V_{S30} = 3000 ± 300 m/sec.

** σ is a generic standard deviation that represents either $\phi_{\ln\kappa_{0,ref}}$ or $\sigma_{\ln\kappa_{0,ref}}$

8.2 RECOMMENDED ALEATORY VARIABILITY IN REFERENCE-ROCK SITE KAPPA

The natural log standard deviations of 0.45 and 0.47 (with and without including the Monticello Reservoir recordings) that were derived from the κ_0 estimates in Table 1 are considered primarily to be an estimate of aleatory uncertainty related to local variations in site conditions for sites generally classified as CENA hard rock ($V_{S30} > 2000$ m/sec at the surface). These standard deviations also account to some extent for the epistemic uncertainty related to differences in assumed methods and seismological and geophysical parameters used to estimate κ_0. In order to minimize any components of epistemic uncertainty, the aleatory component of the variability in $\kappa_{0,ref}$ was taken from other studies that minimize epistemic uncertainty [Schneider et al. 1993; Silva and Darragh 1995]. As discussed previously, Schneider et al. [1993] estimated κ_0 for 20 soft-rock and firm-rock sites from recordings of the 1989 Loma Prieta, California, earthquake using the response spectral fitting approach (their Model 0). Using these estimates, an aleatory natural log standard deviation of 0.42 was determined in this study (see section on *Uncertainty in Site Kappa*). Silva and Darragh [1995] used the same method to estimate κ_0 for 16 hard-rock sites in CENA. Using these estimates of κ_0, an aleatory natural log standard deviation of 0.43 was determined in this study. Based on these two studies, and considering the standard deviation derived from the estimates in Table 1, the GWG recommended an aleatory natural log standard deviation ($\phi_{\ln\kappa_{0,ref}}$) of 0.43 for $\kappa_{0,ref}$ (Table 11).

8.3 RECOMMENDED EPISTEMIC UNCERTAINTY IN REFERENCE-ROCK SITE KAPPA

Epistemic uncertainty in $\kappa_{0,ref}$ was estimated from the standard error of the mean of the natural log κ_0 using the same studies that were used to estimate aleatory uncertainty. The estimates of the natural log standard errors from Schneider et al. [1993] and Silva and Darragh [1995], and from the estimates in Table 1, have an average value of approximately 0.12. This estimate of the epistemic standard deviation is generally void of uncertainty due to the different methods and trade-offs in the seismological and geophysical parameters used in the general inversion methods. Therefore, the GWG recommended that this value of uncertainty be used to represent epistemic uncertainty in $\kappa_{0,ref}$ ($\varepsilon_{\ln\kappa_{0,ref}}$) when such uncertainties are incorporated in the simulations used to develop GMPEss in order to avoid the double counting of uncertainty (Table 11).

The results of Edwards et al. [2011] provide a means of estimating the epistemic component of standard deviation that incorporates uncertainty in the trade-off of the seismological and geophysical parameters used in the ground motion simulations. These authors inverted the Fourier amplitude spectra of thousands of recordings in Switzerland to determine the value of κ_0 at 83 soft-rock and hard-rock sites. A single set of source, path, and site-amplification parameters was used in the inversions, which shifts the uncertainty in these parameters to the estimate of κ_0. Some of these sites had several hundred recordings, which allowed a stable estimate of the κ_0 distribution. They found that the aleatory standard deviations of κ_0 for individual recording sites were very large, which, for the smaller values of κ_0, represented standard deviations that were significantly larger than their mean. Nonetheless, the standard errors of the mean values of κ_0 at these sites can be used to estimate epistemic uncertainty that incorporates uncertainties in source, path, and site-amplification effects. Using the results from their Method 2, an average natural log standard error of approximately 0.20 was determined in this study from the data given in Table 2 of Edwards et al. [2011]. Based on these results, the GWG recommended that this value be used to represent the epistemic uncertainty in $\kappa_{0,ref}$ ($\varepsilon_{\ln\kappa_{0,ref}}$) when uncertainty in input parameters are not incorporated in the simulations that are used to develop GMPEs (Table 11).

8.4 VALIDATION OF RECOMMENDED REFERENCE-ROCK SITE KAPPA

Figure 5 shows a histogram of the κ_0 estimates listed in Table 1 that clearly indicates a median value of around 0.006 sec. Although there are too few values in Table 1 to clearly define a probability density function, a comparison of the resulting aleatory cumulative lognormal distribution of $\kappa_{0,ref}$ recommended in this study ($\bar{\kappa}_{0,ref} = 0.006$ sec, $\phi_{\ln \kappa_{0,ref}} = 0.43$) with the empirical cumulative distribution of κ_0 derived from the data in Table 1 given in Figure 6 shows at least that the recommended cumulative lognormal distribution is not inconsistent with the data. As a result of their derivation from seismological and geophysical models, the estimates in Table 1 are necessarily model dependent, which adds to their scatter. However, there is no study that has systematically looked at the model dependence of κ_0.

Finally, Figure 7 compares the recommended distribution of $\kappa_{0,ref}$ in this study with the predictions of κ_0 from the $\kappa_0 - V_{S30}$ relationships summarized in Table 7 [Silva et al. 1999; Chandler et al. 2006; Van Houtte et al. 2011; Edwards 2012]. Although there are very few values of κ_0 at sites corresponding to the reference-rock *S*-wave velocity, an extrapolation of these relationships to this velocity ($V_{s,ref} = 3000 \pm 300$ m/sec) brackets the recommended value of $\bar{\kappa}_{0,ref}$ from Table 11 and falls within the total (aleatory plus epistemic) 95th-percentile confidence interval of $\kappa_{0,ref}$. The Lin-Lin relationship of Edwards [2012] just falls within this interval at the minimum value of $V_{s,ref}$ (2700 m/sec), although it falls below this interval at the median value of $V_{s,ref}$.

Based on the information provided in this study, the GWG believes that the median, distribution, and uncertainty recommended for reference-rock site kappa in this report represents the center, body, and range of the technical defensible interpretations of the wider scientific community as required in the SSHAC guidelines [Budnitz et al. 1997; NRC 2012]. According to Figure 1 in Campbell [2009], the two standard-deviation range of $\kappa_{0,ref}$ recommended in this study corresponds to a factor of two or more range in Fourier spectral amplitudes at frequencies exceeding 10 Hz.

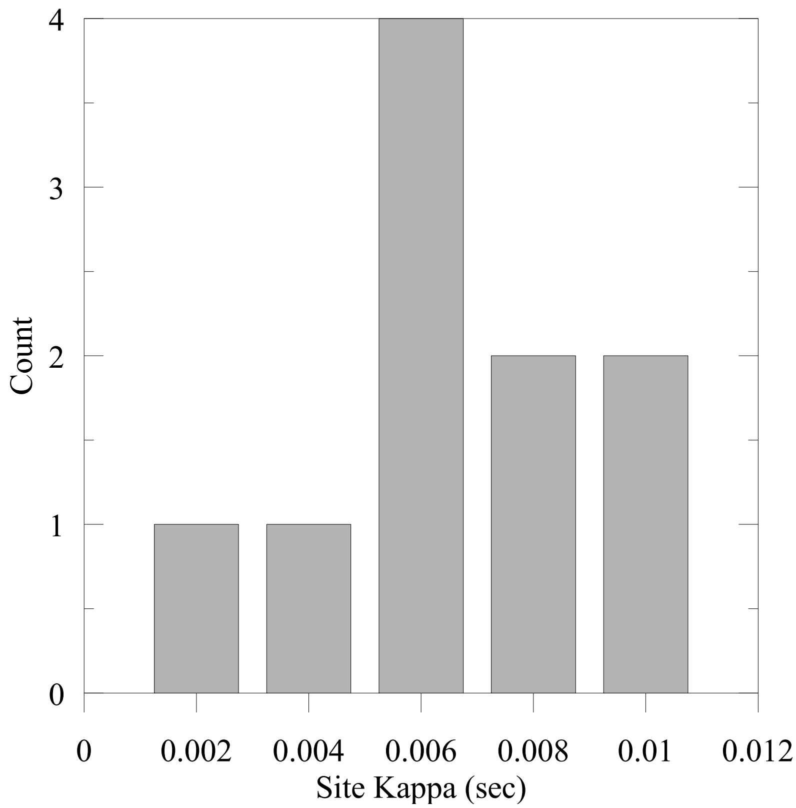

Figure 5 **Histogram of the CENA hard-rock site kappa (κ_0) estimates listed in Table 1 indicating a median value of 0.006 sec, consistent with the median value of CENA reference-rock site kappa recommended in this study $(\kappa_{0,\mathrm{ref}} = 0.006\ \mathrm{sec})$.**

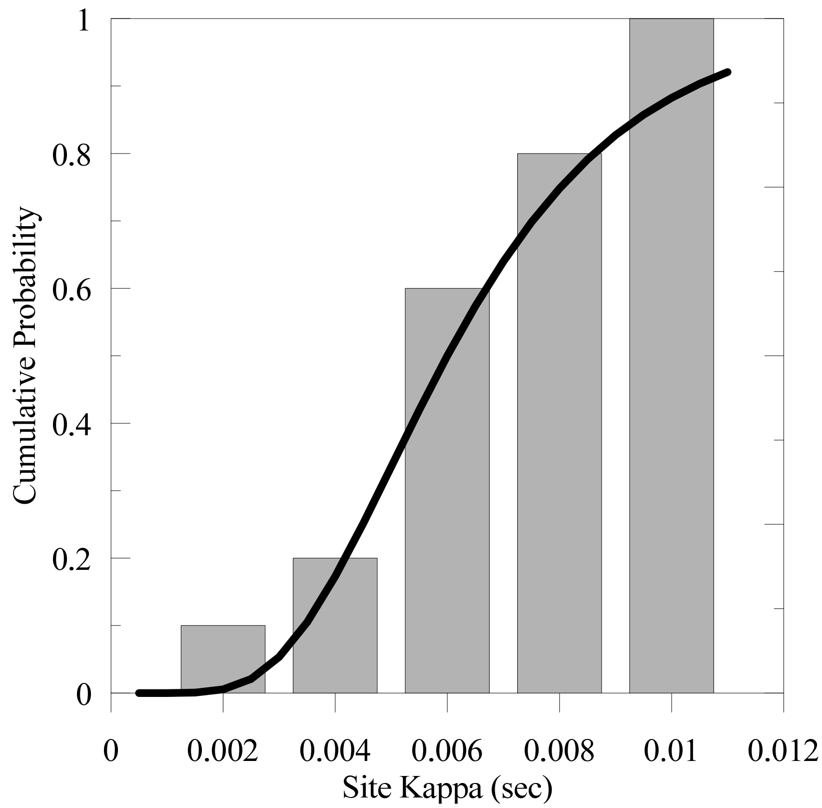

Figure 6 **Histogram of cumulative CENA hard-rock site kappa $\left(\kappa_0\right)$ estimates listed in Table 1 compared to the cumulative lognormal distribution of CENA reference-rock site kappa recommended in this study $\left(\kappa_{0,ref} = 0.006 \text{ sec}\right)$ and $\left(\phi_{\kappa_{0,ref}} = 0.43\right)$.**

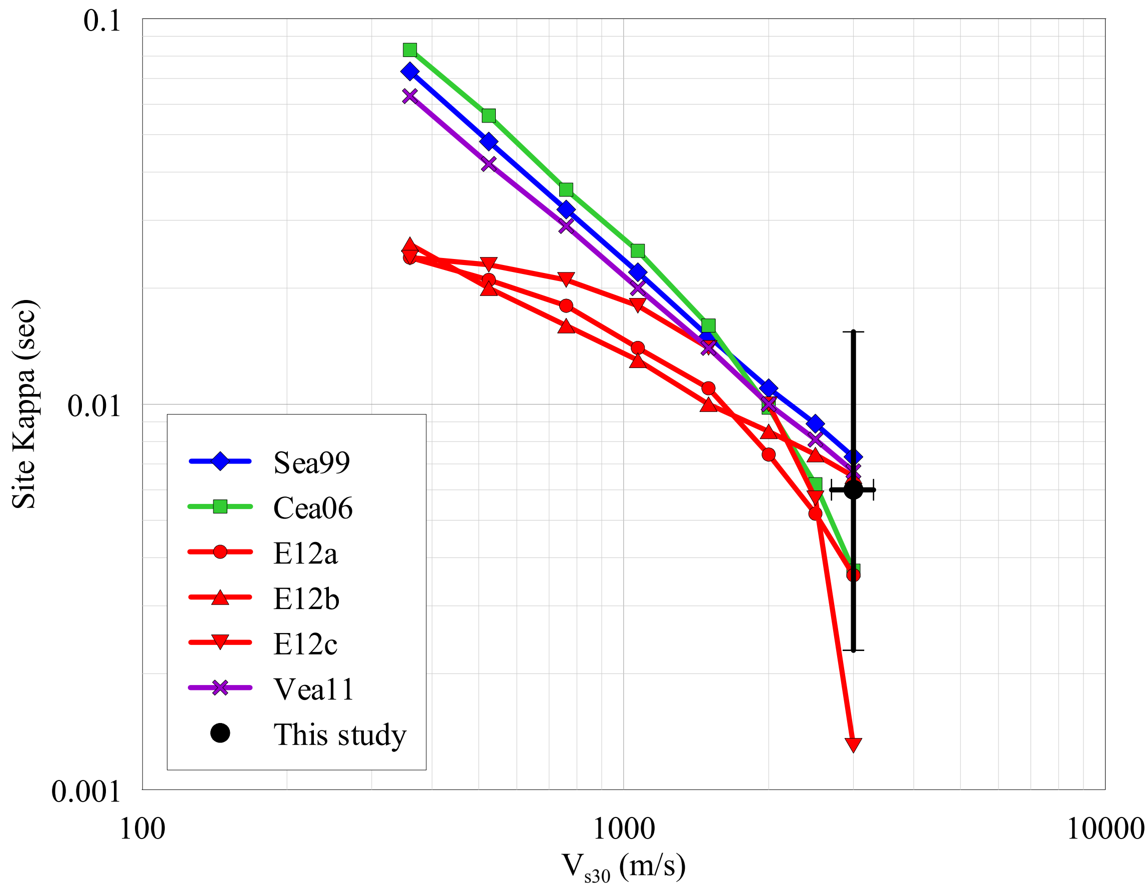

Figure 7 **A comparison of estimates of site kappa (κ_0) from selected $\kappa_0 - V_{S30}$ relationships with the values recommended in this study for the reference-rock *S*-wave velocity $(V_{S,ref})$ of 3000 ± 300 m/sec recommended by the NGA-East Geotechnical Working Group [Hashash et al. 2014a,b]. Abbreviations are the same as in Figure 7. The vertical error bar represents the 95th-percentile confidence internal (plus and minus two standard deviations) of the total distribution of the reference-rock site kappa ($\kappa_{0,ref}$) that includes epistemic uncertainty in source, path, and site-amplification effects.**

9 Future Research

There are a number of issues that were uncovered in this study related to the estimation of κ_0 that can only be resolved with additional research. These issues impact the reliability of the recommended distribution of $\kappa_{0,ref}$ and should be addressed in future studies. These issues include, but are not necessarily limited to, the following items:

1. There are a very limited number of available κ_0 estimates for CENA hard-rock sites, or, for that matter, any hard-rock sites in stable continental regions throughout the world. Additional studies should be conducted to estimate κ_0 for the CENA and worldwide ground motion recordings that are being compiled as part of the NGA-East Project and that are available from other sources.
2. It is not clear what type of probability distribution should be used to characterize uncertainty in κ_0 and whether this distribution should be different for the aleatory and epistemic components of uncertainty. The additional estimates of κ_0 provided in item 1 would help to constrain this distribution.
3. The basis for the standard deviation of κ_0 and how it should be divided between its aleatory and epistemic components of uncertainty is problematic. Additional studies should be conducted to better constrain these standard deviations.
4. This study is based on data primarily from southeastern Canada and northeastern U.S. and does not address what the median value of κ_0 and its uncertainty should be for reference rock in other areas of CENA, such as the carbonate platform regions of CENA, which are common in the Midwest region of North America.
5. This study only considers the shear-wave site attenuation parameter κ_0. Additional studies are needed to characterize the site attenuation parameter for compression waves.

REFERENCES

Abercrombie R.E. (1998). A summary of attenuation measurements from borehole recordings of earthquakes: The 10 Hz transition problem, *Pure Applied Geophys.*, 153(2-4): 475–487.

Aki K. (1980). Scattering and attenuation of shear waves in the lithosphere, *J. Geophys. Res.*, 85(B11): 6496–6504.

Aki K., Chouet B. (1975). Origin of coda waves–Source, attenuation, and scattering effects, *J. Geophys. Res.*, 80(23): 3322–3342.

Allen T.I. (2012). *Stochastic Gound-Motion Prediction Equations for Southeastern Australian Earthquakes Using Updated Source and Attenuation Parameters, Record 2012/69*, Department of Resources, Energy and Tourism, Geoscience Australia. Canberra, Australia.

Anderson D.L., Ben-Menahem A., Archambeau C.B. (1965). Attenuation of seismic energy in the upper mantle, *J. Geophys. Res.*, 70(6): 1441–1448.

Anderson J.G. (1986). Implication of attenuation for studies of the earthquake source, In: *Earthquake Source Mechanics, Geophysics Monograph Series, Vol. 37*, S. Das, J. Boatwright, and C.H. Scholz (Eds.), pp. 311–318, American Geophysical Union. Washington, D.C.

Anderson J.G. (1991). A preliminary descriptive model for the distance dependence of the spectral decay parameter in southern California, *Bull. Seismol. Soc. Am.,* 81(6): 2186–2193.

Anderson J.G., Hough S.E. (1984). A model for the shape of the Fourier amplitude spectrum of acceleration at high frequencies, *Bull. Seismol. Soc. Am.,* 74(5): 1969–1993.

Anderson J.G., Lee Y., Zeng Y., Day S. (1996). Control of strong motion by the upper 30 meters, *Bull. Seismol. Soc. Am.,* 86(6): 1749–1759.

ANSI (2008). *Probabilistic Seismic Hazards Analysis, ANSI Standard ANSI/ANS 2.29-2008*, American National Standards Institute. Washington, D.C.

Aster R.C., Shearer P.M. (1991). High-frequency borehole seismograms recorded in the San Jacinto Fault Zone, southern California. Part 2. Attenuation and site effects, *Bull. Seismol. Soc. Am.,* 81(4): 1081–1100.

Atkinson G.M. Boore D.M. (2006). Earthquake ground-motion prediction equations for eastern North America, *Bull. Seismol. Soc. Am.,* 96(6): 2181–2205.

Atkinson G.M. (1984). Attenuation of strong ground motion in Canada from a random vibrations approach, *Bull. Seismol. Soc. Am.,* 74(6): 2629–2653.

Atkinson G.M. (1995). Attenuation and source parameters of earthquakes in the Cascadia region, *Bull. Seismol. Soc. Am.,* 85(5): 1327-1342.

Atkinson G.M. (1996). The high-frequency shape of the source spectrum for earthquakes in eastern and western Canada, *Bull. Seismol. Soc. Am.,* 86(1A): 106–112.

Atkinson G.M. (2004). Empirical attenuation of ground-motion spectral amplitudes in southeastern Canada and the northeastern United States, *Bull. Seismol. Soc. Am.,* 94(3): 1079–1095.

Atkinson G.M. (2005). Ground motions for earthquakes in southwestern British Columbia and northwestern Washington: Crustal, in-slab, and offshore events, *Bull. Seismol. Soc. Am.,* 95(3): 1027–1044.

Atkinson G.M., Cassidy J.F. (2000). Integrated use of seismograph and strong-motion data to determine soil amplification: Response of the Fraser River Delta to the Duvall and Georgia Strait earthquakes, *Bull. Seismol. Soc. Am.,* 90(4): 1028–1040.

Atkinson G.M., Silva W.J. (1997). An empirical study of earthquake source spectra for California earthquakes, *Bull. Seismol. Soc. Am.,* 87(1): 97–113.

Barton N. (2007). *Rock Quality, Seismic Velocity, Attenuation and Anisotropy*, Taylor & Francis. London.

Bay F., Fäh D., Malagnini L., Giardini D. (2003). Spectral shear-wave ground-motion scaling in Switzerland, *Bull. Seismol. Soc. Am.,* 93(1): 414–429.

Bay F., Wiemer S., Fäh D., Giardini D. (2005). Predictive ground motion scaling in Switzerland: Best estimates and uncertainties, *J. Seismology*, 9(2): 223−240.

Beresnev I.A., Atkinson G.M. (1997). Shear-wave velocity survey of seismographic sites in eastern Canada: Calibration of empirical regression method of estimating site response, *Seismol. Res. Lett.*, 68(6): 981−987.

Beresnev I.A., Atkinson G. M. (1999). Generic finite-fault model for ground-motion prediction in eastern North America, *Bull. Seismol. Soc. Am.,* 89(3): 608−625.

Boore D.M. (1983). Stochastic simulation of high-frequency ground motions based on seismological models of the radiated spectra, *Bull. Seismol. Soc. Am.,* 73(6): 1865−1894.

Boore D.M. (1986). Short-period *P*- and *S*-wave radiation from large earthquakes: implications for spectral scaling relations, *Bull. Seismol. Soc. Am.,* 76(1): 43-64.

Boore D.M. (2003). Prediction of ground motion using the stochastic method, *Pure Applied Geophys.*, 160: 635−676.

Boore D.M., Atkinson G.M. (1987). Stochastic prediction of ground motion and spectral response parameters for hard-rock sites in eastern North America, *Bull. Seismol. Soc. Am.,* 77(2): 440-467.

Boore D.M., Joyner W.B. (1997). Site amplifications for generic rock sites, *Bull. Seismol. Soc. Am.,* 87(2): 327−341.

Boore D.M., Joyner W.B., Fumal T.E. (1993). Estimation of response spectra and peak accelerations from western United States earthquakes: An interim report*, U.S.G.S. Open-File Report 93-509*. U.S. Geological Survey, 72 pgs.

Brune J.N. (1970). Tectonic stress and the spectra of seismic shear waves from earthquakes, *J. Geophys. Res.*, 75(26): 4997−5009.

Brune J.N. (1971). Correction: Tectonic stress and the spectra of seismic shear waves from earthquakes, *J. Geophys. Res.*, 76: 5002.

BSSC (2009). *NEHRP Recommended Seismic Provisions for New Buildings and Other Structures (FEMA P-750), 2009 Edition*, Building Seismic Safety Commission, National Institute of Building Sciences. Washington, D.C.

Budnitz R.J., Apostolakis G., Boore D.M., Cluff L.S. Coppersmith K.J., Cornell C.A., Morris P.A. (1997). *Recommendations for Probabilistic Seismic Hazard Analysis: Guidance on Uncertainty and Use of Experts, NUREG/CR-6372*, U.S. Nuclear Regulatory Commission. Washington, D.C.

Campbell K.W. (2003). Prediction of strong ground motion using the hybrid empirical method and its use in the development of ground-motion (attenuation) relations in Eastern North America, *Bull. Seismol. Soc. Am.,* 93(3): 1012−1033.

Campbell K.W. (2009). Estimates of shear-wave Q and κ_0 for unconsolidated and semiconsolidated sediments in Eastern North America, *Bull. Seismol. Soc. Am.,* 99(4): 2365−2392.

Campillo M., Plantet J.L., Bouchon M. (1985). Frequency-dependent attenuation in the crust beneath central France from LG waves−Data analysis and numerical modeling, *Bull. Seismol. Soc. Am.,* 75(5): 1395−1411.

Castro, R.R., Trojani L., Monachesi G., Mucciarelli M. and Cattaneo M. (2000). The spectral decay parameter κ in the region of Umbria-Marche, Italy, *J. Geophys. Res.*, 105(B10): 23811−23823.

Chandler A.M., Lam N.T.K., Tsang H.H. (2005). Shear wave velocity modelling in crustal rock for seismic hazard analysis, *Soil Dyn. Earthq. Eng.*, 25(2): 167−185.

Chandler A.M., Lam N.T.K., Tsang H.H. (2006). Near-surface attenuation modelling based on rock shear-wave velocity profile, *Soil Dyn. Earthq. Eng.*, 26(11): 1004−1014.

Chapman M.C., Talwani P., Cannon R.C. (2003). Ground-motion attenuation in the Atlantic Coastal Plain near Charleston, South Carolina, *Bull. Seismol. Soc. Am.,* 93(3): 998−1011.

Chiou B.S.-J., Darragh R.B., Gregor N., Silva W.J. (2008). NGA project strong-motion database, *Earthq. Spectra*, 24(1): 23−44.

Clowes R.M., Brandon M.T., Green A.G., Yorath C.J., Brown A.S., Kanasewich E.R., Spencer C. (1987). LITHOPROBE−Southern Vancouver Island: Cenozoic subduction complex imaged by deep seismic reflections, *Canadian J. Earth Sci.*, 24(1): 31−51.

Cormier V.F. (1982). The effect of attenuation on seismic body waves, *Bull. Seismol. Soc. Am.,* 72: S169−S200.

Darragh R.B., Green R.K., Turcott F.T. (1989). *Spectral Characteristics of Small Magnitude Earthquakes with Application to Western and Eastern North American Tectonic Environments: Surface Motions and Depth Effects, Miscellaneous Paper Gl-89-16,* U.S. Army Corps of Engineers, Waterways Experiment Station. Vicksburg, MI.

Dainty A.M. (1981). A scattering model to explain seismic *Q* observations in the lithosphere between 1 and 30 Hz, *Geophy. Res. Lett.*, 8(11): 1126−1128.

DOE (2011). *Natural Phenomena Hazards and Design and Evaluation Criteria for Department of Energy Facilities, Standard DOE-STD-1020-2011*, U.S. Department of Energy. Washington, D.C.

Douglas J., Gehl P., Bonilla L.F., Ǵlis C. (2010). A κ model for mainland France, *Pure Applied Geophys.,* 167(11): 1303−1315.

Drouet S., Cotton F., Guéguen P. (2010). V_{S30}, κ, regional attenuation and M_W from accelerograms: Application to magnitude 3–5 French earthquakes, *Geophys. J. Inter*., 182(2): 880−898.

Edwards B. (2012). *Site Specific Kappa, Technical Report SED/PRP/R/035b/20120410*, Swiss Seismological Service. Zurich, Switzerland.

Edwards B., Fäh D., Giardini D. (2011). Attenuation of seismic shear wave energy in Switzerland, *Geophys. J. Inter.,* 185(2): 967−984.

EPRI (1993). Method and guidelines for estimating earthquake ground motion in eastern North America, In: *Guidelines for Determining Design Basis Ground Motions, EPRI TR-102293, Vol. 1*, Electric Power Research Institute. Palo Alto, CA.

Fäh D., Fritsche S., Poggi V., Gassner-Stamm G., Kästli P., Burjanek J., Zweifel P., Barman S., Clinton J., Keller L., Renault P., Heuberger S. (2009). *Determination of Site Information for Seismic Stations in Switzerland, Technical Report SED/PRP/R/004/20090831*, Swiss Seismological Service. Zurich, Switzerland.

Fehler M., Roberts P., Fairbanks T. (1988). A temporal change in coda wave attenuation observed during an eruption of Mount St. Helens, *J. Geophys. Res.*, 93(B5): 4367−4373.

Fletcher J.B., Fumal T., Hsi-Ping L., Carroll L.C. (1990). Near-surface velocities and attenuation at two boreholes near Anza, California, from logging data, *Bull. Seismol. Soc. Am.,* 80(4): 807−831.

Frankel A., Mueller C., Perkins D., Barnhard T., Leyendecker E., Safak E., Hanson S., Dickman N., Hopper M. (1996). *National Seismic Hazard Maps: Documentation June 1996, U.S.G.S. Open-File Report 96-532*, U.S. Geological Survey, 69 pgs.

Frankel A., Wennerberg L. (1987). Energy-flux model of seismic coda: Separation of scattering and intrinsic attenuation, *Bull. Seismol. Soc. Am.,* 77(4): 1223−1251.

Futterman W.I. (1962). Dispersive body waves, *J. Geophys. Res.*, 67(13): 5279−5291.

Gentili S., Franceschina G. (2011). High frequency attenuation of shear waves in the southeastern Alps and northern Dinarides, *Geophys. J. Inter.,* 185(3): 1393−1416.

Halldorsson B., Papageorgiou A.S. (2005). Calibration of the specific barrier model to earthquakes of different tectonic regions, *Bull. Seismol. Soc. Am.,* 95(4): 1276−1300.

Hanks T.C. (1982). f_{max}, *Bull. Seismol. Soc. Am.,* 72(6A): 1867−1879.

Hanks T.C., McGuire R.K. (1981). The character of high frequency strong ground motion, *Bull. Seismol. Soc. Am.,* 71(6): 2071−2095.

Hashash Y.M.A., Kottke A.R., Stewart J.P., Campbell K.W., Kim B., Moss C., Nikolaou S., Rathje E.M., Silva W.J. (2014a). Reference rock site condition for central and eastern North America, *Bull. Seismol. Soc. Am.,* 104(2): 684−701.

Hashash Y.M.A., Kottke A.R., Stewart J.P., Campbell K.W., Kim B., Rathje E.M., Silva W.J., Nikolaou S., Moss C. (2014b). *Reference Rock Site Condition for Central and Eastern North America, Part I – Velocity Definition, PEER Report No. 2013-08*, Pacific Earthquake Engineering Research Center, University of California. Berkeley, CA

Hough S.E., Anderson J.G. (1988). High-frequency spectra observed at Anza, California: Implications for *Q* structure, *Bull. Seismol. Soc. Am.,* 78(2): 692−707.

Hough S.E., Anderson J.G., Brune J., Vernon F. III, Berger J., Fletcher J., Haar L., Hanks T., Baker L. (1988). Attenuation near Anza, California, *Bull. Seismol. Soc. Am.,* 78(2): 672−691.

Hunter J., Harris J., Britton J. (1997). *Compressional and Shear Wave Interval Velocity Data for Quaternary Sediments in the Fraser River Delta from Multichannel Seismic Reflection Surveys, Geological Survey of Canada Open File Report 3325*, Natural Resources Canada. Ottawa, Canada.

IAEA (2010). *Seismic Hazards in Site Evaluation for Nuclear Installations, IAEA Safety Standards Series No. SSG-9*, International Atomic Energy Agency. Vienna, Austria.

IGPP (2001). *Global Crustal Model CRUST2.0,* Institute of Geophysics and Planetary Physics, University of California. San Diego, CA, http://mahi.ucsd.edu/Gabi/rem.dir/crust/crust2.html.

Johnston D.H., Toksöz M.N. (1980). Thermal cracking and amplitude dependent attenuation, *J. Geophys. Res.*, 85(B2): 937−942.

Johnston D.H., Toksöz M.N., Timur A. (1979). Attenuation of seismic waves in dry and saturated rocks − Part II. Mechanism, *Geophys.*, 44(4): 691−711.

Joyner W.B., Warrick R.E., Fumal T.E. (1981). The effect of Quaternary alluvium on strong ground motion in the Coyote Lake, California, earthquake of 1979, *Bull. Seismol. Soc. Am.,* 71(4): 1333−1349.

Kanamori H. (1967). Spectrum of short-period core phases in relation to the attenuation in the mantle, *J. Geophys. Res.*, 72(8): 2181−2186.

Kang I.B., McMechan G.A. (1994). Separation of intrinsic and scattering *Q* based on frequency-dependent amplitude ratios of transmitted waves, *J. Geophys. Res.*, 99(B12): 23875−23885.

Kinoshita S. (2008). Deep-borehole-measured Q_P and Q_S attenuation for two Kanto sediment layer sites, *Bull. Seismol. Soc. Am.,* 98(1): 463−468.

Knopoff L. (1964). *Q*, *Reviews of Geophys. Earth Phys.,* 2(4): 625−660.

Lay T., Wallace T.C. (1995). *Modern Global Seismology*, Academic Press. San Diego, CA.

McGuire R.K. (2004). *Seismic Hazard and Risk Analysis, Monograph No. MNO-10*, Earthquake Engineering Research Institute. Oakland, CA.

Morasca P., Malagnini L., Akinci A., Spallarossa D., Herrmann R.B. (2006). Ground-motion scaling in the western Alps, *J. Seismology*, 10(3): 315−333.

Morozov I.B. (2008). Geometrical attenuation, frequency dependence of *Q*, and the absorption band problem, *Geophys. J. Inter.*, 175(1): 239−252.

Morozov I.B. (2009). Thirty years of confusion around 'Scattering *Q*'? *Seismol. Res. Lett.*, 80(1): 5−7.

NRC (2007). *A Performance-Based Approach to Define the Site-Specific Earthquake Ground Motion, Regulatory Guide 1.208*, U.S. Nuclear Regulatory Commission. Washington, D.C.

NRC (2012). *Practical Implementation Guidelines for SSHAC Level 3 and 4 Hazard Studies, NUREG-2117*, U.S. Nuclear Regulatory Commission. Washington, D.C.

Oth A., Bindi D., Parolai S., di Giacomo D. (2011). Spectral analysis of K-NET and KiK-net data in Japan. Part II. On attenuation characteristics, source spectra, and site response of borehole and surface stations, *Bull. Seismol. Soc. Am.,* 101(2): 667−687.

Ou G.B., Herrmann R.B. (1990). A statistical model for ground motion produced by earthquakes at local and regional distances, *Bull. Seismol. Soc. Am.,* 80(6A): 1397−1417.

Papageorgiou A.S., Aki K. (1983). A specific barrier model for the quantitative description of inhomogeneous faulting and the prediction of strong ground motion. Part 2. Applications of the model, *Bull. Seismol. Soc. Am.,* 73(4): 953–978.

Petersen M.D., Frankel A.D., Harmsen S.C., Mueller C.S., Haller K.M., Wheeler R.L., Wesson R.L., Zeng Y., Boyd O.S., Perkins D.M., Luco N., Field E.H., Wills C.J., Rukstales K.S. (2008). *Documentation for the 2008 Update of the United States National Seismic Hazard Maps, U.S.G.S. Open-File Report 2008-1128*, U.S. Geological Survey, 61 pgs.

Poggi V., Edwards B., Fäh D. (2011). Derivation of a reference shear-wave velocity model from empirical site amplification, *Bull. Seismol. Soc. Am.,* 101(1): 258–274.

Pulli J.J. (1984). Attenuation of coda waves in New England, *Bull. Seismol. Soc. Am.,* 74(4): 1149–1166.

Purvance M.D., Anderson J.G. (2003). A comprehensive study of the observed spectral decay in strong-motion accelerations recorded in Guerrero, Mexico, *Bull. Seismol. Soc. Am.,* 93(2): 600–611.

Sato H., Fehler M., Wu R.S. (2002). Scattering and attenuation of seismic waves in the lithosphere, In: *International Handbook of Earthquake & Engineering Seismology, Part A,* W.H.K. Lee, H. Kanamori, P.C. Jennings and C. Kisslinger (Eds.), Academic Press. San Diego, CA.

Schneider J.F., Silva W.J., Stark C. (1993). Ground motion model for the 1989 M 6.9 Loma Prieta earthquake including effects of source, path, and site, *Earthq. Spectra*, 9(2): 251–287.

Silva W.J., Darragh R.B., Gregor N.N., Martin G., Abrahamson N.A., Kircher C. (1999). *Reassessment of Site Coefficients and Near-Fault Factors for Building Code Provisions, NEHRP External Research Program, Final Technical Report, U.S. Geological Survey Award No. 98HQGR1010*, Pacific Engineering & Analysis. El Cerrito, CA.

Silva W.J., Abrahamson N.A., Toro G.R., Costantino C. (1997). *Description and Validation of the Stochastic Ground Motion Model, Report to Brookhaven National Laboratory*, Associated Universities, Inc., Upton, New York. Pacfiic Engineering & Analysis, El Cerrito, CA.

Silva W.J., Darragh R.B. (1995). *Engineering Characterization of Earthquake Strong Ground Motion Recorded at Rock Sites, EPRI TR-102262*, Electric Power Research Institute. Palo Alto, CA.

Silva W.J., Darragh R.B., Stark C., Wong I., Stepp J.C., Schneider J., Choiu B.S-J. (1990). A methodology to estimate design response spectra in the near-source region of large earthquakes using the band-limited-white-noise ground motion model, *Proceedings, 4th U.S. National Conference on Earthquake Engineering*, pp. 487–494. Palm Springs, CA.

Silva W.J., Green R.K. (1989). Magnitude and distance scaling of response spectral shapes for rock sites with applications to North American tectonic environment, *Earthq. Spectra,* 5(3): 591–624.

Silva W.J., Gregor N., Darragh R.B. (2002). *Development of Regional Hard-Rock Attenuation Relations for Central and Eastern North America*, Pacific Engineering & Analysis. El Cerrito, CA.

Somerville P., Collins N., Abrahamson N.A., Graves R., Saikia C. (2001). *Ground Motion Attenuation Relations for the Central and Eastern United States, NEHRP External Research Program, Final Technical Report, U.S. Geological Survey Award Number: 99HQGR0098*, URS Group, Inc. Pasadena, CA.

Spence G.D., Clowes R.M., Ellis R.M. (1985). Seismic structure across the active subduction zone of western Canada, *J. Geophys. Res.*, 90(B8): 6754–6772.

Tavakoli B., Pezeshk S. (2005). Empirical-stochastic ground-motion prediction for eastern North America, *Bull. Seismol. Soc. Am.,* 95(6): 2283–2296.

Toro G.R., Abrahamson N.A., Schneider J.F. (1997). Model of strong ground motions from earthquakes in central and eastern North America: Best estimates and uncertainties, *Seismol. Res. Lett.*, 68(1): 41–57.

Toro G.R., McGuire R.K. (1987). An investigation into earthquake ground motion characteristics in eastern North America, *Bull. Seismol. Soc. Am.,* 77(2): 468–489.

Van Houtte C., Drouet S., Cotton F. (2011). Analysis of the origins of κ (kappa) to compute hard rock to rock adjustment factors for GMPEs, *Bull. Seismol. Soc. Am.,* 101(6): 2926–2941.

Vernon F.L., Pavlis G.L., Owens T.J., McNamara D.E., Anderson P.N. (1998). Near-surface scattering effects observed with a high-frequency phased array at Pinyon Flats, California, *Bull. Seismol. Soc. Am.,* 88(6): 1548–1560.

PEER REPORTS

PEER reports are available as a free PDF download from http://peer.berkeley.edu/publications/peer_reports_complete.html. Printed hard copies of PEER reports can be ordered directly from our printer by following the instructions at http://peer.berkeley.edu/publications/peer_reports.html. For other related questions about the PEER Report Series, contact the Pacific Earthquake Engineering Research Center, 325 Davis Hall mail code 1792, Berkeley, CA 94720. Tel.: (510) 642-3437; Fax: (510) 665-1655; Email: peer_editor@berkeley.edu

PEER 2014/12 *Reference-Rock Site Conditions for Central and Eastern North America: Part II – Attenuation (Kappa) Definition.* Kenneth W. Campbell, Youssef M.A. Hashash, Byungmin Kim, Albert R. Kottke, Ellen M. Rathje, Walter J. Silva, and Jonathan P. Stewart. August 2014.

PEER 2014/11 *Reference-Rock Site Conditions for Central and Eastern North America: Part I - Velocity Definition.* Youssef M.A. Hashash, Albert R. Kottke, Jonathan P. Stewart, Kenneth W. Campbell, Byungmin Kim, Ellen M. Rathje, Walter J. Silva, Sissy Nikolaou, and Cheryl Moss. August 2014.

PEER 2014/10 *Evaluation of Collapse and Non-Collapse of Parallel Bridges Affected by Liquefaction and Lateral Spreading*. Benjamin Turner, Scott J. Brandenberg, and Jonathan P. Stewart. August 2014.

PEER 2014/09 *PEER Arizona Strong-Motion Database and GMPEs Evaluation*. Tadahiro Kishida, Robert E. Kayen, Olga-Joan Ktenidou, Walter J. Silva, Robert B. Darragh, and Jennie Watson-Lamprey. June 2014.

PEER 2014/08 *Unbonded Pretensioned Bridge Columns with Rocking Detail*. Jeffrey A. Schaefer, Bryan Kennedy, Marc O. Eberhard, John F. Stanton. June 2014.

PEER 2014/07 *Northridge 20 Symposium Summary Report: Impacts, Outcomes, and Next Steps*. May 2014.

PEER 2014/06 *Report of the Tenth Planning Meeting of NEES/E-Defense Collaborative Research on Earthquake Engineering*. December 2013.

PEER 2014/05 *Seismic Velocity Site Characterization of Thirty-One Chilean Seismometer Stations by Spectral Analysis of Surface Wave Dispersion.* Robert Kayen, Brad D. Carkin, Skye Corbet, Camilo Pinilla, Allan Ng, Edward Gorbis, and Christine Truong. April 2014.

PEER 2014/04 *Effect of Vertical Acceleration on Shear Strength of Reinforced Concrete Columns.* Hyerin Lee and Khalid M. Mosalam. April 2014.

PEER 2014/03 *Retest of Thirty-Year-Old Neoprene Isolation Bearings.* James M. Kelly and Niel C. Van Engelen. March 2014.

PEER 2014/02 *Theoretical Development of Hybrid Simulation Applied to Plate Structures.* Ahmed A. Bakhaty, Khalid M. Mosalam, and Sanjay Govindjee. January 2014.

PEER 2014/01 *Performance-Based Seismic Assessment of Skewed Bridges.* Peyman Kaviani, Farzin Zareian, and Ertugrul Taciroglu. January 2014.

PEER 2013/26 *Urban Earthquake Engineering. Proceedings of the U.S.-Iran Seismic Workshop.* December 2013.

PEER 2013/25 *Earthquake Engineering for Resilient Communities: 2013 PEER Internship Program Research Report Collection.* Heidi Tremayne (Editor), Stephen A. Mahin (Editor), Jorge Archbold Monterossa, Matt Brosman, Shelly Dean, Katherine deLaveaga, Curtis Fong, Donovan Holder, Rakeeb Khan, Elizabeth Jachens, David Lam, Daniela Martinez Lopez, Mara Minner, Geffen Oren, Julia Pavicic, Melissa Quinonez, Lorena Rodriguez, Sean Salazar, Kelli Slaven, Vivian Steyert, Jenny Taing, and Salvador Tena. December 2013.

PEER 2013/24 *NGA-West2 Ground Motion Prediction Equations for Vertical Ground Motions.* September 2013.

PEER 2013/23 *Coordinated Planning and Preparedness for Fire Following Major Earthquakes.* Charles Scawthorn. November 2013.

PEER 2013/22 *GEM-PEER Task 3 Project: Selection of a Global Set of Ground Motion Prediction Equations.* Jonathan P. Stewart, John Douglas, Mohammad B. Javanbarg, Carola Di Alessandro, Yousef Bozorgnia, Norman A. Abrahamson, David M. Boore, Kenneth W. Campbell, Elise Delavaud, Mustafa Erdik and Peter J. Stafford. December 2013.

PEER 2013/21 *Seismic Design and Performance of Bridges with Columns on Rocking Foundations.* Grigorios Antonellis and Marios Panagiotou. September 2013.

PEER 2013/20 *Experimental and Analytical Studies on the Seismic Behavior of Conventional and Hybrid Braced Frames.* Jiun-Wei Lai and Stephen A. Mahin. September 2013.

PEER 2013/19 *Toward Resilient Communities: A Performance-Based Engineering Framework for Design and Evaluation of the Built Environment.* Michael William Mieler, Bozidar Stojadinovic, Robert J. Budnitz, Stephen A. Mahin and Mary C. Comerio. September 2013.

PEER 2013/18 *Identification of Site Parameters that Improve Predictions of Site Amplification.* Ellen M. Rathje and Sara Navidi. July 2013.

PEER 2013/17 *Response Spectrum Analysis of Concrete Gravity Dams Including Dam-Water-Foundation Interaction.* Arnkjell Løkke and Anil K. Chopra. July 2013.

PEER 2013/16 *Effect of hoop reinforcement spacing on the cyclic response of large reinforced concrete special moment frame beams.* Marios Panagiotou, Tea Visnjic, Grigorios Antonellis, Panagiotis Galanis, and Jack P. Moehle. June 2013.

PEER 2013/15 *A Probabilistic Framework to Include the Effects of Near-Fault Directivity in Seismic Hazard Assessment.* Shrey Kumar Shahi, Jack W. Baker. October 2013.

PEER 2013/14 *Hanging-Wall Scaling using Finite-Fault Simulations.* Jennifer L. Donahue and Norman A. Abrahamson. September 2013.

PEER 2013/13 *Semi-Empirical Nonlinear Site Amplification and its Application in NEHRP Site Factors.* Jonathan P. Stewart and Emel Seyhan. November 2013.

PEER 2013/12 *Nonlinear Horizontal Site Response for the NGA-West2 Project.* Ronnie Kamai, Norman A. Abramson, Walter J. Silva. May 2013.

PEER 2013/11 *Epistemic Uncertainty for NGA-West2 Models.* Linda Al Atik and Robert R. Youngs. May 2013.

PEER 2013/10 *NGA-West 2 Models for Ground-Motion Directionality.* Shrey K. Shahi and Jack W. Baker. May 2013.

PEER 2013/09 *Final Report of the NGA-West2 Directivity Working Group.* Paul Spudich, Jeffrey R. Bayless, Jack W. Baker, Brian S.J. Chiou, Badie Rowshandel, Shrey Shahi, and Paul Somerville. May 2013.

PEER 2013/08 *NGA-West2 Model for Estimating Average Horizontal Values of Pseudo-Absolute Spectral Accelerations Generated by Crustal Earthquakes.* I. M. Idriss. May 2013.

PEER 2013/07 *Update of the Chiou and Youngs NGA Ground Motion Model for Average Horizontal Component of Peak Ground Motion and Response Spectra.* Brian Chiou and Robert Youngs. May 2013.

PEER 2013/06 *NGA-West2 Campbell-Bozorgnia Ground Motion Model for the Horizontal Components of PGA, PGV, and 5%-Damped Elastic Pseudo-Acceleration Response Spectra for Periods Ranging from 0.01 to 10 sec.* Kenneth W. Campbell and Yousef Bozorgnia. May 2013.

PEER 2013/05 *NGA-West 2 Equations for Predicting Response Spectral Accelerations for Shallow Crustal Earthquakes.* David M. Boore, Jonathan P. Stewart, Emel Seyhan, Gail M. Atkinson. May 2013.

PEER 2013/04 *Update of the AS08 Ground-Motion Prediction Equations Based on the NGA-West2 Data Set.* Norman Abrahamson, Walter Silva, and Ronnie Kamai. May 2013.

PEER 2013/03 *PEER NGA-West2 Database.* Timothy D. Ancheta, Robert B. Darragh, Jonathan P. Stewart, Emel Seyhan, Walter J. Silva, Brian S.J. Chiou, Katie E. Wooddell, Robert W. Graves, Albert R. Kottke, David M. Boore, Tadahiro Kishida, and Jennifer L. Donahue. May 2013.

PEER 2013/02 *Hybrid Simulation of the Seismic Response of Squat Reinforced Concrete Shear Walls.* Catherine A. Whyte and Bozidar Stojadinovic. May 2013.

PEER 2013/01 *Housing Recovery in Chile: A Qualitative Mid-program Review.* Mary C. Comerio. February 2013.

PEER 2012/08 *Guidelines for Estimation of Shear Wave Velocity.* Bernard R. Wair, Jason T. DeJong, and Thomas Shantz. December 2012.

PEER 2012/07 *Earthquake Engineering for Resilient Communities: 2012 PEER Internship Program Research Report Collection.* Heidi Tremayne (Editor), Stephen A. Mahin (Editor), Collin Anderson, Dustin Cook, Michael Erceg, Carlos Esparza, Jose Jimenez, Dorian Krausz, Andrew Lo, Stephanie Lopez, Nicole McCurdy, Paul Shipman, Alexander Strum, Eduardo Vega. December 2012.

PEER 2012/06 *Fragilities for Precarious Rocks at Yucca Mountain.* Matthew D. Purvance, Rasool Anooshehpoor, and James N. Brune. December 2012.

PEER 2012/05 *Development of Simplified Analysis Procedure for Piles in Laterally Spreading Layered Soils.* Christopher R. McGann, Pedro Arduino, and Peter Mackenzie–Helnwein. December 2012.

PEER 2012/04 *Unbonded Pre-Tensioned Columns for Bridges in Seismic Regions.* Phillip M. Davis, Todd M. Janes, Marc O. Eberhard, and John F. Stanton. December 2012.

PEER 2012/03 *Experimental and Analytical Studies on Reinforced Concrete Buildings with Seismically Vulnerable Beam-Column Joints.* Sangjoon Park and Khalid M. Mosalam. October 2012.

PEER 2012/02 *Seismic Performance of Reinforced Concrete Bridges Allowed to Uplift during Multi-Directional Excitation.* Andres Oscar Espinoza and Stephen A. Mahin. July 2012.

PEER 2012/01 *Spectral Damping Scaling Factors for Shallow Crustal Earthquakes in Active Tectonic Regions.* Sanaz Rezaeian, Yousef Bozorgnia, I. M. Idriss, Kenneth Campbell, Norman Abrahamson, and Walter Silva. July 2012.

PEER 2011/10 *Earthquake Engineering for Resilient Communities: 2011 PEER Internship Program Research Report Collection.* Eds. Heidi Faison and Stephen A. Mahin. December 2011.

PEER 2011/09 *Calibration of Semi-Stochastic Procedure for Simulating High-Frequency Ground Motions.* Jonathan P. Stewart, Emel Seyhan, and Robert W. Graves. December 2011.

PEER 2011/08 *Water Supply in regard to Fire Following Earthquake.* Charles Scawthorn. November 2011.

PEER 2011/07 *Seismic Risk Management in Urban Areas. Proceedings of a U.S.-Iran-Turkey Seismic Workshop.* September 2011.

PEER 2011/06 *The Use of Base Isolation Systems to Achieve Complex Seismic Performance Objectives.* Troy A. Morgan and Stephen A. Mahin. July 2011.

PEER 2011/05 *Case Studies of the Seismic Performance of Tall Buildings Designed by Alternative Means.* Task 12 Report for the Tall Buildings Initiative. Jack Moehle, Yousef Bozorgnia, Nirmal Jayaram, Pierson Jones, Mohsen Rahnama, Nilesh Shome, Zeynep Tuna, John Wallace, Tony Yang, and Farzin Zareian. July 2011.

PEER 2011/04 *Recommended Design Practice for Pile Foundations in Laterally Spreading Ground.* Scott A. Ashford, Ross W. Boulanger, and Scott J. Brandenberg. June 2011.

PEER 2011/03 *New Ground Motion Selection Procedures and Selected Motions for the PEER Transportation Research Program.* Jack W. Baker, Ting Lin, Shrey K. Shahi, and Nirmal Jayaram. March 2011.

PEER 2011/02 *A Bayesian Network Methodology for Infrastructure Seismic Risk Assessment and Decision Support.* Michelle T. Bensi, Armen Der Kiureghian, and Daniel Straub. March 2011.

PEER 2011/01 *Demand Fragility Surfaces for Bridges in Liquefied and Laterally Spreading Ground.* Scott J. Brandenberg, Jian Zhang, Pirooz Kashighandi, Yili Huo, and Minxing Zhao. March 2011.

PEER 2010/05 *Guidelines for Performance-Based Seismic Design of Tall Buildings.* Developed by the Tall Buildings Initiative. November 2010.

PEER 2010/04 *Application Guide for the Design of Flexible and Rigid Bus Connections between Substation Equipment Subjected to Earthquakes.* Jean-Bernard Dastous and Armen Der Kiureghian. September 2010.

PEER 2010/03 *Shear Wave Velocity as a Statistical Function of Standard Penetration Test Resistance and Vertical Effective Stress at Caltrans Bridge Sites.* Scott J. Brandenberg, Naresh Bellana, and Thomas Shantz. June 2010.

PEER 2010/02 *Stochastic Modeling and Simulation of Ground Motions for Performance-Based Earthquake Engineering.* Sanaz Rezaeian and Armen Der Kiureghian. June 2010.

PEER 2010/01 *Structural Response and Cost Characterization of Bridge Construction Using Seismic Performance Enhancement Strategies.* Ady Aviram, Božidar Stojadinović, Gustavo J. Parra-Montesinos, and Kevin R. Mackie. March 2010.

PEER 2009/03 *The Integration of Experimental and Simulation Data in the Study of Reinforced Concrete Bridge Systems Including Soil-Foundation-Structure Interaction.* Matthew Dryden and Gregory L. Fenves. November 2009.

PEER 2009/02 *Improving Earthquake Mitigation through Innovations and Applications in Seismic Science, Engineering, Communication, and Response. Proceedings of a U.S.-Iran Seismic Workshop.* October 2009.

PEER 2009/01 *Evaluation of Ground Motion Selection and Modification Methods: Predicting Median Interstory Drift Response of Buildings.* Curt B. Haselton, Ed. June 2009.

PEER 2008/10 *Technical Manual for Strata.* Albert R. Kottke and Ellen M. Rathje. February 2009.

PEER 2008/09 *NGA Model for Average Horizontal Component of Peak Ground Motion and Response Spectra.* Brian S.-J. Chiou and Robert R. Youngs. November 2008.

PEER 2008/08 *Toward Earthquake-Resistant Design of Concentrically Braced Steel Structures.* Patxi Uriz and Stephen A. Mahin. November 2008.

PEER 2008/07 *Using OpenSees for Performance-Based Evaluation of Bridges on Liquefiable Soils.* Stephen L. Kramer, Pedro Arduino, and HyungSuk Shin. November 2008.

PEER 2008/06 *Shaking Table Tests and Numerical Investigation of Self-Centering Reinforced Concrete Bridge Columns.* Hyung IL Jeong, Junichi Sakai, and Stephen A. Mahin. September 2008.

PEER 2008/05 *Performance-Based Earthquake Engineering Design Evaluation Procedure for Bridge Foundations Undergoing Liquefaction-Induced Lateral Ground Displacement.* Christian A. Ledezma and Jonathan D. Bray. August 2008.

PEER 2008/04 *Benchmarking of Nonlinear Geotechnical Ground Response Analysis Procedures.* Jonathan P. Stewart, Annie On-Lei Kwok, Yousseff M. A. Hashash, Neven Matasovic, Robert Pyke, Zhiliang Wang, and Zhaohui Yang. August 2008.

PEER 2008/03 *Guidelines for Nonlinear Analysis of Bridge Structures in California.* Ady Aviram, Kevin R. Mackie, and Božidar Stojadinović. August 2008.

PEER 2008/02 *Treatment of Uncertainties in Seismic-Risk Analysis of Transportation Systems.* Evangelos Stergiou and Anne S. Kiremidjian. July 2008.

PEER 2008/01 *Seismic Performance Objectives for Tall Buildings.* William T. Holmes, Charles Kircher, William Petak, and Nabih Youssef. August 2008.

PEER 2007/12 *An Assessment to Benchmark the Seismic Performance of a Code-Conforming Reinforced Concrete Moment-Frame Building.* Curt Haselton, Christine A. Goulet, Judith Mitrani-Reiser, James L. Beck, Gregory G. Deierlein, Keith A. Porter, Jonathan P. Stewart, and Ertugrul Taciroglu. August 2008.

PEER 2007/11 *Bar Buckling in Reinforced Concrete Bridge Columns.* Wayne A. Brown, Dawn E. Lehman, and John F. Stanton. February 2008.

PEER 2007/10 *Computational Modeling of Progressive Collapse in Reinforced Concrete Frame Structures.* Mohamed M. Talaat and Khalid M. Mosalam. May 2008.

PEER 2007/09 *Integrated Probabilistic Performance-Based Evaluation of Benchmark Reinforced Concrete Bridges.* Kevin R. Mackie, John-Michael Wong, and Božidar Stojadinović. January 2008.

PEER 2007/08 *Assessing Seismic Collapse Safety of Modern Reinforced Concrete Moment-Frame Buildings.* Curt B. Haselton and Gregory G. Deierlein. February 2008.

PEER 2007/07 *Performance Modeling Strategies for Modern Reinforced Concrete Bridge Columns.* Michael P. Berry and Marc O. Eberhard. April 2008.

PEER 2007/06 *Development of Improved Procedures for Seismic Design of Buried and Partially Buried Structures.* Linda Al Atik and Nicholas Sitar. June 2007.

PEER 2007/05 *Uncertainty and Correlation in Seismic Risk Assessment of Transportation Systems.* Renee G. Lee and Anne S. Kiremidjian. July 2007.

PEER 2007/04 *Numerical Models for Analysis and Performance-Based Design of Shallow Foundations Subjected to Seismic Loading.* Sivapalan Gajan, Tara C. Hutchinson, Bruce L. Kutter, Prishati Raychowdhury, José A. Ugalde, and Jonathan P. Stewart. May 2008.

PEER 2007/03 *Beam-Column Element Model Calibrated for Predicting Flexural Response Leading to Global Collapse of RC Frame Buildings.* Curt B. Haselton, Abbie B. Liel, Sarah Taylor Lange, and Gregory G. Deierlein. May 2008.

PEER 2007/02 *Campbell-Bozorgnia NGA Ground Motion Relations for the Geometric Mean Horizontal Component of Peak and Spectral Ground Motion Parameters.* Kenneth W. Campbell and Yousef Bozorgnia. May 2007.

PEER 2007/01 *Boore-Atkinson NGA Ground Motion Relations for the Geometric Mean Horizontal Component of Peak and Spectral Ground Motion Parameters.* David M. Boore and Gail M. Atkinson. May. May 2007.

PEER 2006/12 *Societal Implications of Performance-Based Earthquake Engineering.* Peter J. May. May 2007.

PEER 2006/11 *Probabilistic Seismic Demand Analysis Using Advanced Ground Motion Intensity Measures, Attenuation Relationships, and Near-Fault Effects.* Polsak Tothong and C. Allin Cornell. March 2007.

PEER 2006/10 *Application of the PEER PBEE Methodology to the I-880 Viaduct.* Sashi Kunnath. February 2007.

PEER 2006/09 *Quantifying Economic Losses from Travel Forgone Following a Large Metropolitan Earthquake.* James Moore, Sungbin Cho, Yue Yue Fan, and Stuart Werner. November 2006.

PEER 2006/08 *Vector-Valued Ground Motion Intensity Measures for Probabilistic Seismic Demand Analysis.* Jack W. Baker and C. Allin Cornell. October 2006.

PEER 2006/07 *Analytical Modeling of Reinforced Concrete Walls for Predicting Flexural and Coupled–Shear-Flexural Responses.* Kutay Orakcal, Leonardo M. Massone, and John W. Wallace. October 2006.

PEER 2006/06 *Nonlinear Analysis of a Soil-Drilled Pier System under Static and Dynamic Axial Loading.* Gang Wang and Nicholas Sitar. November 2006.

PEER 2006/05 *Advanced Seismic Assessment Guidelines.* Paolo Bazzurro, C. Allin Cornell, Charles Menun, Maziar Motahari, and Nicolas Luco. September 2006.

PEER 2006/04 *Probabilistic Seismic Evaluation of Reinforced Concrete Structural Components and Systems.* Tae Hyung Lee and Khalid M. Mosalam. August 2006.

PEER 2006/03 *Performance of Lifelines Subjected to Lateral Spreading.* Scott A. Ashford and Teerawut Juirnarongrit. July 2006.

PEER 2006/02 *Pacific Earthquake Engineering Research Center Highway Demonstration Project.* Anne Kiremidjian, James Moore, Yue Yue Fan, Nesrin Basoz, Ozgur Yazali, and Meredith Williams. April 2006.

PEER 2006/01 *Bracing Berkeley. A Guide to Seismic Safety on the UC Berkeley Campus.* Mary C. Comerio, Stephen Tobriner, and Ariane Fehrenkamp. January 2006.

PEER 2005/16 *Seismic Response and Reliability of Electrical Substation Equipment and Systems.* Junho Song, Armen Der Kiureghian, and Jerome L. Sackman. April 2006.

PEER 2005/15 *CPT-Based Probabilistic Assessment of Seismic Soil Liquefaction Initiation.* R. E. S. Moss, R. B. Seed, R. E. Kayen, J. P. Stewart, and A. Der Kiureghian. April 2006.

PEER 2005/14 *Workshop on Modeling of Nonlinear Cyclic Load-Deformation Behavior of Shallow Foundations.* Bruce L. Kutter, Geoffrey Martin, Tara Hutchinson, Chad Harden, Sivapalan Gajan, and Justin Phalen. March 2006.

PEER 2005/13 *Stochastic Characterization and Decision Bases under Time-Dependent Aftershock Risk in Performance-Based Earthquake Engineering.* Gee Liek Yeo and C. Allin Cornell. July 2005.

PEER 2005/12 *PEER Testbed Study on a Laboratory Building: Exercising Seismic Performance Assessment.* Mary C. Comerio, editor. November 2005.

PEER 2005/11 *Van Nuys Hotel Building Testbed Report: Exercising Seismic Performance Assessment.* Helmut Krawinkler, editor. October 2005.

PEER 2005/10 *First NEES/E-Defense Workshop on Collapse Simulation of Reinforced Concrete Building Structures.* September 2005.

PEER 2005/09 *Test Applications of Advanced Seismic Assessment Guidelines.* Joe Maffei, Karl Telleen, Danya Mohr, William Holmes, and Yuki Nakayama. August 2006.

PEER 2005/08 *Damage Accumulation in Lightly Confined Reinforced Concrete Bridge Columns.* R. Tyler Ranf, Jared M. Nelson, Zach Price, Marc O. Eberhard, and John F. Stanton. April 2006.

PEER 2005/07 *Experimental and Analytical Studies on the Seismic Response of Freestanding and Anchored Laboratory Equipment.* Dimitrios Konstantinidis and Nicos Makris. January 2005.

PEER 2005/06 *Global Collapse of Frame Structures under Seismic Excitations.* Luis F. Ibarra and Helmut Krawinkler. September 2005.

PEER 2005//05 *Performance Characterization of Bench- and Shelf-Mounted Equipment.* Samit Ray Chaudhuri and Tara C. Hutchinson. May 2006.

PEER 2005/04 *Numerical Modeling of the Nonlinear Cyclic Response of Shallow Foundations.* Chad Harden, Tara Hutchinson, Geoffrey R. Martin, and Bruce L. Kutter. August 2005.

PEER 2005/03 *A Taxonomy of Building Components for Performance-Based Earthquake Engineering.* Keith A. Porter. September 2005.

PEER 2005/02 *Fragility Basis for California Highway Overpass Bridge Seismic Decision Making.* Kevin R. Mackie and Božidar Stojadinović. June 2005.

PEER 2005/01 *Empirical Characterization of Site Conditions on Strong Ground Motion.* Jonathan P. Stewart, Yoojoong Choi, and Robert W. Graves. June 2005.

PEER 2004/09 *Electrical Substation Equipment Interaction: Experimental Rigid Conductor Studies.* Christopher Stearns and André Filiatrault. February 2005.

PEER 2004/08 *Seismic Qualification and Fragility Testing of Line Break 550-kV Disconnect Switches.* Shakhzod M. Takhirov, Gregory L. Fenves, and Eric Fujisaki. January 2005.

PEER 2004/07 *Ground Motions for Earthquake Simulator Qualification of Electrical Substation Equipment.* Shakhzod M. Takhirov, Gregory L. Fenves, Eric Fujisaki, and Don Clyde. January 2005.

PEER 2004/06 *Performance-Based Regulation and Regulatory Regimes.* Peter J. May and Chris Koski. September 2004.

PEER 2004/05 *Performance-Based Seismic Design Concepts and Implementation: Proceedings of an International Workshop.* Peter Fajfar and Helmut Krawinkler, editors. September 2004.

PEER 2004/04 *Seismic Performance of an Instrumented Tilt-up Wall Building.* James C. Anderson and Vitelmo V. Bertero. July 2004.

PEER 2004/03 *Evaluation and Application of Concrete Tilt-up Assessment Methodologies.* Timothy Graf and James O. Malley. October 2004.

PEER 2004/02 *Analytical Investigations of New Methods for Reducing Residual Displacements of Reinforced Concrete Bridge Columns.* Junichi Sakai and Stephen A. Mahin. August 2004.

PEER 2004/01 *Seismic Performance of Masonry Buildings and Design Implications.* Kerri Anne Taeko Tokoro, James C. Anderson, and Vitelmo V. Bertero. February 2004.

PEER 2003/18 *Performance Models for Flexural Damage in Reinforced Concrete Columns.* Michael Berry and Marc Eberhard. August 2003.

PEER 2003/17 *Predicting Earthquake Damage in Older Reinforced Concrete Beam-Column Joints.* Catherine Pagni and Laura Lowes. October 2004.

PEER 2003/16 *Seismic Demands for Performance-Based Design of Bridges.* Kevin Mackie and Božidar Stojadinović. August 2003.

PEER 2003/15 *Seismic Demands for Nondeteriorating Frame Structures and Their Dependence on Ground Motions.* Ricardo Antonio Medina and Helmut Krawinkler. May 2004.

PEER 2003/14 *Finite Element Reliability and Sensitivity Methods for Performance-Based Earthquake Engineering.* Terje Haukaas and Armen Der Kiureghian. April 2004.

PEER 2003/13 *Effects of Connection Hysteretic Degradation on the Seismic Behavior of Steel Moment-Resisting Frames.* Janise E. Rodgers and Stephen A. Mahin. March 2004.

PEER 2003/12 *Implementation Manual for the Seismic Protection of Laboratory Contents: Format and Case Studies.* William T. Holmes and Mary C. Comerio. October 2003.

PEER 2003/11 *Fifth U.S.-Japan Workshop on Performance-Based Earthquake Engineering Methodology for Reinforced Concrete Building Structures.* February 2004.

PEER 2003/10 *A Beam-Column Joint Model for Simulating the Earthquake Response of Reinforced Concrete Frames.* Laura N. Lowes, Nilanjan Mitra, and Arash Altoontash. February 2004.

PEER 2003/09 *Sequencing Repairs after an Earthquake: An Economic Approach.* Marco Casari and Simon J. Wilkie. April 2004.

PEER 2003/08 *A Technical Framework for Probability-Based Demand and Capacity Factor Design (DCFD) Seismic Formats.* Fatemeh Jalayer and C. Allin Cornell. November 2003.

PEER 2003/07 *Uncertainty Specification and Propagation for Loss Estimation Using FOSM Methods.* Jack W. Baker and C. Allin Cornell. September 2003.

PEER 2003/06 *Performance of Circular Reinforced Concrete Bridge Columns under Bidirectional Earthquake Loading.* Mahmoud M. Hachem, Stephen A. Mahin, and Jack P. Moehle. February 2003.

PEER 2003/05 *Response Assessment for Building-Specific Loss Estimation.* Eduardo Miranda and Shahram Taghavi. September 2003.

PEER 2003/04 *Experimental Assessment of Columns with Short Lap Splices Subjected to Cyclic Loads.* Murat Melek, John W. Wallace, and Joel Conte. April 2003.

PEER 2003/03 *Probabilistic Response Assessment for Building-Specific Loss Estimation.* Eduardo Miranda and Hesameddin Aslani. September 2003.

PEER 2003/02 *Software Framework for Collaborative Development of Nonlinear Dynamic Analysis Program.* Jun Peng and Kincho H. Law. September 2003.

PEER 2003/01 *Shake Table Tests and Analytical Studies on the Gravity Load Collapse of Reinforced Concrete Frames.* Kenneth John Elwood and Jack P. Moehle. November 2003.

PEER 2002/24 *Performance of Beam to Column Bridge Joints Subjected to a Large Velocity Pulse.* Natalie Gibson, André Filiatrault, and Scott A. Ashford. April 2002.

PEER 2002/23 *Effects of Large Velocity Pulses on Reinforced Concrete Bridge Columns.* Greg L. Orozco and Scott A. Ashford. April 2002.

PEER 2002/22 *Characterization of Large Velocity Pulses for Laboratory Testing.* Kenneth E. Cox and Scott A. Ashford. April 2002.

PEER 2002/21 *Fourth U.S.-Japan Workshop on Performance-Based Earthquake Engineering Methodology for Reinforced Concrete Building Structures.* December 2002.

PEER 2002/20 *Barriers to Adoption and Implementation of PBEE Innovations.* Peter J. May. August 2002.

PEER 2002/19 *Economic-Engineered Integrated Models for Earthquakes: Socioeconomic Impacts.* Peter Gordon, James E. Moore II, and Harry W. Richardson. July 2002.

PEER 2002/18 *Assessment of Reinforced Concrete Building Exterior Joints with Substandard Details.* Chris P. Pantelides, Jon Hansen, Justin Nadauld, and Lawrence D. Reaveley. May 2002.

PEER 2002/17 *Structural Characterization and Seismic Response Analysis of a Highway Overcrossing Equipped with Elastomeric Bearings and Fluid Dampers: A Case Study.* Nicos Makris and Jian Zhang. November 2002.

PEER 2002/16 *Estimation of Uncertainty in Geotechnical Properties for Performance-Based Earthquake Engineering.* Allen L. Jones, Steven L. Kramer, and Pedro Arduino. December 2002.

PEER 2002/15 *Seismic Behavior of Bridge Columns Subjected to Various Loading Patterns.* Asadollah Esmaeily-Gh. and Yan Xiao. December 2002.

PEER 2002/14 *Inelastic Seismic Response of Extended Pile Shaft Supported Bridge Structures.* T.C. Hutchinson, R.W. Boulanger, Y.H. Chai, and I.M. Idriss. December 2002.

PEER 2002/13 *Probabilistic Models and Fragility Estimates for Bridge Components and Systems.* Paolo Gardoni, Armen Der Kiureghian, and Khalid M. Mosalam. June 2002.

PEER 2002/12 *Effects of Fault Dip and Slip Rake on Near-Source Ground Motions: Why Chi-Chi Was a Relatively Mild M7.6 Earthquake.* Brad T. Aagaard, John F. Hall, and Thomas H. Heaton. December 2002.

PEER 2002/11 *Analytical and Experimental Study of Fiber-Reinforced Strip Isolators*. James M. Kelly and Shakhzod M. Takhirov. September 2002.

PEER 2002/10 *Centrifuge Modeling of Settlement and Lateral Spreading with Comparisons to Numerical Analyses***.** Sivapalan Gajan and Bruce L. Kutter. January 2003.

PEER 2002/09 *Documentation and Analysis of Field Case Histories of Seismic Compression during the 1994 Northridge, California, Earthquake.* Jonathan P. Stewart, Patrick M. Smith, Daniel H. Whang, and Jonathan D. Bray. October 2002.

PEER 2002/08 *Component Testing, Stability Analysis and Characterization of Buckling-Restrained Unbonded Braces™.* Cameron Black, Nicos Makris, and Ian Aiken. September 2002.

PEER 2002/07 *Seismic Performance of Pile-Wharf Connections.* Charles W. Roeder, Robert Graff, Jennifer Soderstrom, and Jun Han Yoo. December 2001.

PEER 2002/06 *The Use of Benefit-Cost Analysis for Evaluation of Performance-Based Earthquake Engineering Decisions.* Richard O. Zerbe and Anthony Falit-Baiamonte. September 2001.

PEER 2002/05 *Guidelines, Specifications, and Seismic Performance Characterization of Nonstructural Building Components and Equipment*. André Filiatrault, Constantin Christopoulos, and Christopher Stearns. September 2001.

PEER 2002/04 *Consortium of Organizations for Strong-Motion Observation Systems and the Pacific Earthquake Engineering Research Center Lifelines Program: Invited Workshop on Archiving and Web Dissemination of Geotechnical Data, 4–5 October 2001*. September 2002.

PEER 2002/03 *Investigation of Sensitivity of Building Loss Estimates to Major Uncertain Variables for the Van Nuys Testbed.* Keith A. Porter, James L. Beck, and Rustem V. Shaikhutdinov. August 2002.

PEER 2002/02 *The Third U.S.-Japan Workshop on Performance-Based Earthquake Engineering Methodology for Reinforced Concrete Building Structures*. July 2002.

PEER 2002/01 *Nonstructural Loss Estimation: The UC Berkeley Case Study.* Mary C. Comerio and John C. Stallmeyer. December 2001.

PEER 2001/16 *Statistics of SDF-System Estimate of Roof Displacement for Pushover Analysis of Buildings.* Anil K. Chopra, Rakesh K. Goel, and Chatpan Chintanapakdee. December 2001.

PEER 2001/15 *Damage to Bridges during the 2001 Nisqually Earthquake.* R. Tyler Ranf, Marc O. Eberhard, and Michael P. Berry. November 2001.

PEER 2001/14 *Rocking Response of Equipment Anchored to a Base Foundation.* Nicos Makris and Cameron J. Black. September 2001.

PEER 2001/13 *Modeling Soil Liquefaction Hazards for Performance-Based Earthquake Engineering.* Steven L. Kramer and Ahmed-W. Elgamal. February 2001.

PEER 2001/12 *Development of Geotechnical Capabilities in OpenSees.* Boris Jeremić. September 2001.

PEER 2001/11 *Analytical and Experimental Study of Fiber-Reinforced Elastomeric Isolators*. James M. Kelly and Shakhzod M. Takhirov. September 2001.

PEER 2001/10 *Amplification Factors for Spectral Acceleration in Active Regions.* Jonathan P. Stewart, Andrew H. Liu, Yoojoong Choi, and Mehmet B. Baturay. December 2001.

PEER 2001/09 *Ground Motion Evaluation Procedures for Performance-Based Design.* Jonathan P. Stewart, Shyh-Jeng Chiou, Jonathan D. Bray, Robert W. Graves, Paul G. Somerville, and Norman A. Abrahamson. September 2001.

PEER 2001/08 *Experimental and Computational Evaluation of Reinforced Concrete Bridge Beam-Column Connections for Seismic Performance.* Clay J. Naito, Jack P. Moehle, and Khalid M. Mosalam. November 2001.

PEER 2001/07 *The Rocking Spectrum and the Shortcomings of Design Guidelines.* Nicos Makris and Dimitrios Konstantinidis. August 2001.

PEER 2001/06 *Development of an Electrical Substation Equipment Performance Database for Evaluation of Equipment Fragilities.* Thalia Agnanos. April 1999.

PEER 2001/05 *Stiffness Analysis of Fiber-Reinforced Elastomeric Isolators.* Hsiang-Chuan Tsai and James M. Kelly. May 2001.

PEER 2001/04 *Organizational and Societal Considerations for Performance-Based Earthquake Engineering.* Peter J. May. April 2001.

PEER 2001/03 *A Modal Pushover Analysis Procedure to Estimate Seismic Demands for Buildings: Theory and Preliminary Evaluation.* Anil K. Chopra and Rakesh K. Goel. January 2001.

PEER 2001/02 *Seismic Response Analysis of Highway Overcrossings Including Soil-Structure Interaction.* Jian Zhang and Nicos Makris. March 2001.

PEER 2001/01 *Experimental Study of Large Seismic Steel Beam-to-Column Connections.* Egor P. Popov and Shakhzod M. Takhirov. November 2000.

PEER 2000/10 *The Second U.S.-Japan Workshop on Performance-Based Earthquake Engineering Methodology for Reinforced Concrete Building Structures.* March 2000.

PEER 2000/09 *Structural Engineering Reconnaissance of the August 17, 1999 Earthquake: Kocaeli (Izmit), Turkey.* Halil Sezen, Kenneth J. Elwood, Andrew S. Whittaker, Khalid Mosalam, John J. Wallace, and John F. Stanton. December 2000.

PEER 2000/08 *Behavior of Reinforced Concrete Bridge Columns Having Varying Aspect Ratios and Varying Lengths of Confinement.* Anthony J. Calderone, Dawn E. Lehman, and Jack P. Moehle. January 2001.

PEER 2000/07 *Cover-Plate and Flange-Plate Reinforced Steel Moment-Resisting Connections.* Taejin Kim, Andrew S. Whittaker, Amir S. Gilani, Vitelmo V. Bertero, and Shakhzod M. Takhirov. September 2000.

PEER 2000/06 *Seismic Evaluation and Analysis of 230-kV Disconnect Switches.* Amir S. J. Gilani, Andrew S. Whittaker, Gregory L. Fenves, Chun-Hao Chen, Henry Ho, and Eric Fujisaki. July 2000.

PEER 2000/05 *Performance-Based Evaluation of Exterior Reinforced Concrete Building Joints for Seismic Excitation.* Chandra Clyde, Chris P. Pantelides, and Lawrence D. Reaveley. July 2000.

PEER 2000/04 *An Evaluation of Seismic Energy Demand: An Attenuation Approach.* Chung-Che Chou and Chia-Ming Uang. July 1999.

PEER 2000/03 *Framing Earthquake Retrofitting Decisions: The Case of Hillside Homes in Los Angeles.* Detlof von Winterfeldt, Nels Roselund, and Alicia Kitsuse. March 2000.

PEER 2000/02 *U.S.-Japan Workshop on the Effects of Near-Field Earthquake Shaking.* Andrew Whittaker, ed. July 2000.

PEER 2000/01 *Further Studies on Seismic Interaction in Interconnected Electrical Substation Equipment.* Armen Der Kiureghian, Kee-Jeung Hong, and Jerome L. Sackman. November 1999.

PEER 1999/14 *Seismic Evaluation and Retrofit of 230-kV Porcelain Transformer Bushings.* Amir S. Gilani, Andrew S. Whittaker, Gregory L. Fenves, and Eric Fujisaki. December 1999.

PEER 1999/13 *Building Vulnerability Studies: Modeling and Evaluation of Tilt-up and Steel Reinforced Concrete Buildings.* John W. Wallace, Jonathan P. Stewart, and Andrew S. Whittaker, editors. December 1999.

PEER 1999/12 *Rehabilitation of Nonductile RC Frame Building Using Encasement Plates and Energy-Dissipating Devices.* Mehrdad Sasani, Vitelmo V. Bertero, James C. Anderson. December 1999.

PEER 1999/11 *Performance Evaluation Database for Concrete Bridge Components and Systems under Simulated Seismic Loads.* Yael D. Hose and Frieder Seible. November 1999.

PEER 1999/10 *U.S.-Japan Workshop on Performance-Based Earthquake Engineering Methodology for Reinforced Concrete Building Structures.* December 1999.

PEER 1999/09 *Performance Improvement of Long Period Building Structures Subjected to Severe Pulse-Type Ground Motions.* James C. Anderson, Vitelmo V. Bertero, and Raul Bertero. October 1999.

PEER 1999/08 *Envelopes for Seismic Response Vectors.* Charles Menun and Armen Der Kiureghian. July 1999.

PEER 1999/07 *Documentation of Strengths and Weaknesses of Current Computer Analysis Methods for Seismic Performance of Reinforced Concrete Members.* William F. Cofer. November 1999.

PEER 1999/06 *Rocking Response and Overturning of Anchored Equipment under Seismic Excitations.* Nicos Makris and Jian Zhang. November 1999.

PEER 1999/05 *Seismic Evaluation of 550 kV Porcelain Transformer Bushings.* Amir S. Gilani, Andrew S. Whittaker, Gregory L. Fenves, and Eric Fujisaki. October 1999.

PEER 1999/04 *Adoption and Enforcement of Earthquake Risk-Reduction Measures.* Peter J. May, Raymond J. Burby, T. Jens Feeley, and Robert Wood.

PEER 1999/03 *Task 3 Characterization of Site Response General Site Categories*. Adrian Rodriguez-Marek, Jonathan D. Bray, and Norman Abrahamson. February 1999.

PEER 1999/02 *Capacity-Demand-Diagram Methods for Estimating Seismic Deformation of Inelastic Structures: SDF Systems*. Anil K. Chopra and Rakesh Goel. April 1999.

PEER 1999/01 *Interaction in Interconnected Electrical Substation Equipment Subjected to Earthquake Ground Motions*. Armen Der Kiureghian, Jerome L. Sackman, and Kee-Jeung Hong. February 1999.

PEER 1998/08 *Behavior and Failure Analysis of a Multiple-Frame Highway Bridge in the 1994 Northridge Earthquake.* Gregory L. Fenves and Michael Ellery. December 1998.

PEER 1998/07 *Empirical Evaluation of Inertial Soil-Structure Interaction Effects.* Jonathan P. Stewart, Raymond B. Seed, and Gregory L. Fenves. November 1998.

PEER 1998/06 *Effect of Damping Mechanisms on the Response of Seismic Isolated Structures.* Nicos Makris and Shih-Po Chang. November 1998.

PEER 1998/05 *Rocking Response and Overturning of Equipment under Horizontal Pulse-Type Motions.* Nicos Makris and Yiannis Roussos. October 1998.

PEER 1998/04 *Pacific Earthquake Engineering Research Invitational Workshop Proceedings, May 14–15, 1998: Defining the Links between Planning, Policy Analysis, Economics and Earthquake Engineering.* Mary Comerio and Peter Gordon. September 1998.

PEER 1998/03 *Repair/Upgrade Procedures for Welded Beam to Column Connections.* James C. Anderson and Xiaojing Duan. May 1998.

PEER 1998/02 *Seismic Evaluation of 196 kV Porcelain Transformer Bushings.* Amir S. Gilani, Juan W. Chavez, Gregory L. Fenves, and Andrew S. Whittaker. May 1998.

PEER 1998/01 *Seismic Performance of Well-Confined Concrete Bridge Columns.* Dawn E. Lehman and Jack P. Moehle. December 2000.

ONLINE PEER REPORTS

The following PEER reports are available by Internet only at http://peer.berkeley.edu/publications/peer_reports_complete.html.

PEER 2012/103 *Performance-Based Seismic Demand Assessment of Concentrically Braced Steel Frame Buildings.* Chui-Hsin Chen and Stephen A. Mahin. December 2012.

PEER 2012/102 *Procedure to Restart an Interrupted Hybrid Simulation: Addendum to PEER Report 2010/103.* Vesna Terzic and Bozidar Stojadinovic. October 2012.

PEER 2012/101 *Mechanics of Fiber Reinforced Bearings.* James M. Kelly and Andrea Calabrese. February 2012.

PEER 2011/107 *Nonlinear Site Response and Seismic Compression at Vertical Array Strongly Shaken by 2007 Niigata-ken Chuetsu-oki Earthquake.* Eric Yee, Jonathan P. Stewart, and Kohji Tokimatsu. December 2011.

PEER 2011/106 *Self Compacting Hybrid Fiber Reinforced Concrete Composites for Bridge Columns.* Pardeep Kumar, Gabriel Jen, William Trono, Marios Panagiotou, and Claudia Ostertag. September 2011.

PEER 2011/105 *Stochastic Dynamic Analysis of Bridges Subjected to Spacially Varying Ground Motions.* Katerina Konakli and Armen Der Kiureghian. August 2011.

PEER 2011/104 *Design and Instrumentation of the 2010 E-Defense Four-Story Reinforced Concrete and Post-Tensioned Concrete Buildings.* Takuya Nagae, Kenichi Tahara, Taizo Matsumori, Hitoshi Shiohara, Toshimi Kabeyasawa, Susumu Kono, Minehiro Nishiyama (Japanese Research Team) and John Wallace, Wassim Ghannoum, Jack Moehle, Richard Sause, Wesley Keller, Zeynep Tuna (U.S. Research Team). June 2011.

PEER 2011/103 *In-Situ Monitoring of the Force Output of Fluid Dampers: Experimental Investigation.* Dimitrios Konstantinidis, James M. Kelly, and Nicos Makris. April 2011.

PEER 2011/102 *Ground-motion prediction equations 1964 - 2010.* John Douglas. April 2011.

PEER 2011/101 *Report of the Eighth Planning Meeting of NEES/E-Defense Collaborative Research on Earthquake Engineering.* Convened by the Hyogo Earthquake Engineering Research Center (NIED), NEES Consortium, Inc. February 2011.

PEER 2010/111 *Modeling and Acceptance Criteria for Seismic Design and Analysis of Tall Buildings.* Task 7 Report for the Tall Buildings Initiative - Published jointly by the Applied Technology Council. October 2010.

PEER 2010/110 *Seismic Performance Assessment and Probabilistic Repair Cost Analysis of Precast Concrete Cladding Systems for Multistory Buildlings.* Jeffrey P. Hunt and Božidar Stojadinovic. November 2010.

PEER 2010/109 *Report of the Seventh Joint Planning Meeting of NEES/E-Defense Collaboration on Earthquake Engineering. Held at the E-Defense, Miki, and Shin-Kobe, Japan, September 18–19, 2009.* August 2010.

PEER 2010/108 *Probabilistic Tsunami Hazard in California.* Hong Kie Thio, Paul Somerville, and Jascha Polet, preparers. October 2010.

PEER 2010/107 *Performance and Reliability of Exposed Column Base Plate Connections for Steel Moment-Resisting Frames.* Ady Aviram, Božidar Stojadinovic, and Armen Der Kiureghian. August 2010.

PEER 2010/106 *Verification of Probabilistic Seismic Hazard Analysis Computer Programs.* Patricia Thomas, Ivan Wong, and Norman Abrahamson. May 2010.

PEER 2010/105 *Structural Engineering Reconnaissance of the April 6, 2009, Abruzzo, Italy, Earthquake, and Lessons Learned.* M. Selim Günay and Khalid M. Mosalam. April 2010.

PEER 2010/104 *Simulating the Inelastic Seismic Behavior of Steel Braced Frames, Including the Effects of Low-Cycle Fatigue.* Yuli Huang and Stephen A. Mahin. April 2010.

PEER 2010/103 *Post-Earthquake Traffic Capacity of Modern Bridges in California.* Vesna Terzic and Božidar Stojadinović. March 2010.

PEER 2010/102 *Analysis of Cumulative Absolute Velocity (CAV) and JMA Instrumental Seismic Intensity (I_{JMA}) Using the PEER–NGA Strong Motion Database.* Kenneth W. Campbell and Yousef Bozorgnia. February 2010.

PEER 2010/101 *Rocking Response of Bridges on Shallow Foundations.* Jose A. Ugalde, Bruce L. Kutter, and Boris Jeremic. April 2010.

PEER 2009/109 *Simulation and Performance-Based Earthquake Engineering Assessment of Self-Centering Post-Tensioned Concrete Bridge Systems.* Won K. Lee and Sarah L. Billington. December 2009.

PEER 2009/108 *PEER Lifelines Geotechnical Virtual Data Center.* J. Carl Stepp, Daniel J. Ponti, Loren L. Turner, Jennifer N. Swift, Sean Devlin, Yang Zhu, Jean Benoit, and John Bobbitt. September 2009.

PEER 2009/107 *Experimental and Computational Evaluation of Current and Innovative In-Span Hinge Details in Reinforced Concrete Box-Girder Bridges: Part 2: Post-Test Analysis and Design Recommendations.* Matias A. Hube and Khalid M. Mosalam. December 2009.

PEER 2009/106 *Shear Strength Models of Exterior Beam-Column Joints without Transverse Reinforcement.* Sangjoon Park and Khalid M. Mosalam. November 2009.

PEER 2009/105 *Reduced Uncertainty of Ground Motion Prediction Equations through Bayesian Variance Analysis.* Robb Eric S. Moss. November 2009.

PEER 2009/104 *Advanced Implementation of Hybrid Simulation.* Andreas H. Schellenberg, Stephen A. Mahin, Gregory L. Fenves. November 2009.

PEER 2009/103 *Performance Evaluation of Innovative Steel Braced Frames.* T. Y. Yang, Jack P. Moehle, and Božidar Stojadinovic. August 2009.

PEER 2009/102 *Reinvestigation of Liquefaction and Nonliquefaction Case Histories from the 1976 Tangshan Earthquake.* Robb Eric Moss, Robert E. Kayen, Liyuan Tong, Songyu Liu, Guojun Cai, and Jiaer Wu. August 2009.

PEER 2009/101 *Report of the First Joint Planning Meeting for the Second Phase of NEES/E-Defense Collaborative Research on Earthquake Engineering.* Stephen A. Mahin et al. July 2009.

PEER 2008/104 *Experimental and Analytical Study of the Seismic Performance of Retaining Structures.* Linda Al Atik and Nicholas Sitar. January 2009.

PEER 2008/103 *Experimental and Computational Evaluation of Current and Innovative In-Span Hinge Details in Reinforced Concrete Box-Girder Bridges. Part 1: Experimental Findings and Pre-Test Analysis.* Matias A. Hube and Khalid M. Mosalam. January 2009.

PEER 2008/102 *Modeling of Unreinforced Masonry Infill Walls Considering In-Plane and Out-of-Plane Interaction.* Stephen Kadysiewski and Khalid M. Mosalam. January 2009.

PEER 2008/101 *Seismic Performance Objectives for Tall Buildings.* William T. Holmes, Charles Kircher, William Petak, and Nabih Youssef. August 2008.

PEER 2007/101 *Generalized Hybrid Simulation Framework for Structural Systems Subjected to Seismic Loading.* Tarek Elkhoraibi and Khalid M. Mosalam. July 2007.

PEER 2007/100 *Seismic Evaluation of Reinforced Concrete Buildings Including Effects of Masonry Infill Walls.* Alidad Hashemi and Khalid M. Mosalam. July 2007.

The Pacific Earthquake Engineering Research Center (PEER) is a multi-institutional research and education center with headquarters at the University of California, Berkeley. Investigators from over 20 universities, several consulting companies, and researchers at various state and federal government agencies contribute to research programs focused on performance-based earthquake engineering.

These research programs aim to identify and reduce the risks from major earthquakes to life safety and to the economy by including research in a wide variety of disciplines including structural and geotechnical engineering, geology/seismology, lifelines, transportation, architecture, economics, risk management, and public policy.

PEER is supported by federal, state, local, and regional agencies, together with industry partners.

PEER Core Institutions:
University of California, Berkeley (Lead Institution)
California Institute of Technology
Oregon State University
Stanford University
University of California, Davis
University of California, Irvine
University of California, Los Angeles
University of California, San Diego
University of Southern California
University of Washington

PEER reports can be ordered at http://peer.berkeley.edu/publications/peer_reports.html or by contacting

Pacific Earthquake Engineering Research Center
University of California, Berkeley
325 Davis Hall, mail code 1792
Berkeley, CA 94720-1792
Tel: 510-642-3437
Fax: 510-642-1655
Email: peer_editor@berkeley.edu

ISSN 1547-0587X